

(19) World Intellectual Property Organization
International Bureau



(43) International Publication Date
5 December 2002 (05.12.2002)

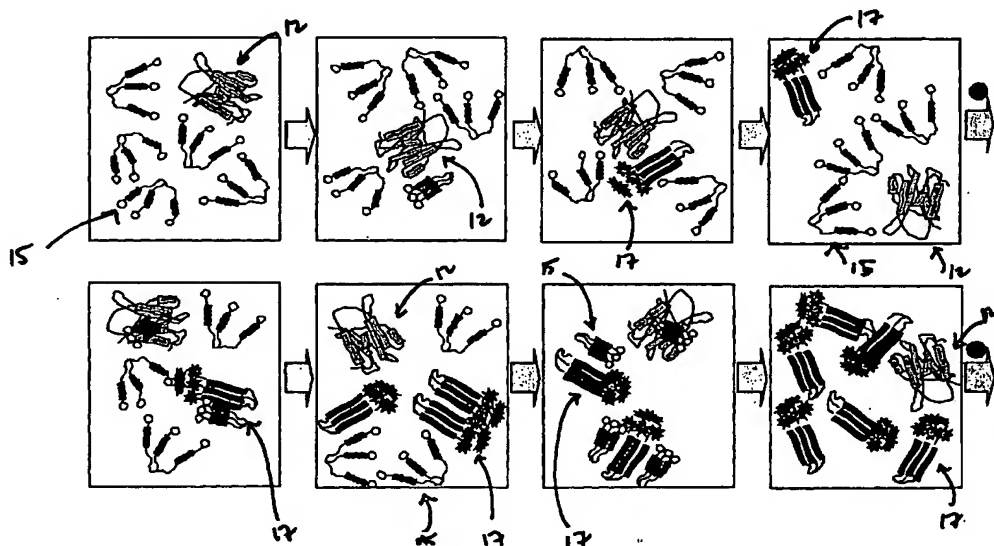
PCT

(10) International Publication Number
WO 02/097444 A2

- (51) International Patent Classification⁷: **G01N 33/68**
- (21) International Application Number: **PCT/US02/17212**
- (22) International Filing Date: **30 May 2002 (30.05.2002)**
- (25) Filing Language: **English**
- (26) Publication Language: **English**
- (30) Priority Data:
60/295,456 **31 May 2001 (31.05.2001)** **US**
- (71) Applicant (for all designated States except US): **ARETE ASSOCIATES [US/US]**; 5000 Van Nuys Boulevard, Suite 420, Sherman Oaks, CA 91403 (US).
- (72) Inventors; and
- (75) Inventors/Applicants (for US only): **ORSER, Cindy [US/US]**; 915 Ridge Drive, McLean, VA 22101 (US). **GROSSET, Anne [US/US]**; 205, route de Bardonnex, CH-1257 La Croix-de-Rozon (CH). **DAVIDSON, Eugene [US/US]**; 5506 Nebraska Avenue, NW, Washington, DC 20015 (US).
- (74) Agent: **LIPPMAN, Peter, L.**; Ashen & Lippman, 4385 Ocean View Boulevard, Montrose, CA 91020 (US).
- (81) Designated States (national): AE, AG, AL, AM, AT, AU, AZ, BA, BB, BG, BR, BY, BZ, CA, CH, CN, CO, CR, CU, CZ, DE, DK, DM, DZ, EC, EE, ES, FI, GB, GD, GE, GH, GM, HR, HU, ID, IL, IN, IS, JP, KE, KG, KP, KR, KZ, LC, LK, LR, LS, LT, LU, LV, MA, MD, MG, MK, MN, MW, MX, MZ, NO, NZ, OM, PH, PL, PT, RO, RU, SD, SE, SG, SI, SK, SL, TJ, TM, TN, TR, TT, TZ, UA, UG, US, UZ, VN, YU, ZA, ZM, ZW.
- (84) Designated States (regional): ARIPO patent (GH, GM, KE, LS, MW, MZ, SD, SL, SZ, TZ, UG, ZM, ZW), Eurasian patent (AM, AZ, BY, KG, KZ, MD, RU, TJ, TM), European patent (AT, BE, CH, CY, DE, DK, ES, FI, FR, GB, GR, IE, IT, LU, MC, NL, PT, SE, TR), OAPI patent (BF, BJ, CF, CG, CI, CM, GA, GN, GQ, GW, ML, MR, NE, SN, TD, TG).
- Published:
— without international search report and to be republished upon receipt of that report

[Continued on next page]

(54) Title: **MISFOLDED PROTEIN SENSOR METHOD**



(57) Abstract: A catalytic conformational sensor method for detecting abnormal proteins and proteinaceous particles. The method is based on the interaction of a peptide fragment or probe with an abnormal proteinaceous particle. The interaction catalyzes transformation of the probe to a predominately beta sheet conformation and allows the probe to bind to the abnormal proteinaceous particle. This in turn, catalyzes propagation of a signal associated with the test sample-bound probe. As a result signals can be propagated even from samples containing very low concentrations of abnormal proteinaceous particles. The peptide probes can be designed to bind to a desired peptide sequence or can even be based on dendrimer structure to control further aggregate propagation.

WO 02/097444 A2



For two-letter codes and other abbreviations, refer to the "Guidance Notes on Codes and Abbreviations" appearing at the beginning of each regular issue of the PCT Gazette.

MISFOLDED PROTEIN SENSOR METHOD

BACKGROUND

1. FIELD OF THE INVENTION

This invention relates generally to a catalytic conformational sensor method and application of such method for detecting proteins and proteinaceous particles; and more particularly to detecting misfolded or disease-associated proteins and proteinaceous particles.

2. RELATED ART

This document claims priority of United States provisional patent application serial number 60/295,456 filed on May 31, 2001, with respect to subject matter therein; said provisional application fully being incorporated herein.

The present invention detects misfolded or abnormal conformations of proteins or peptides such as those contributing to "folding diseases". The "folding diseases" are characterized by proteins with destabilizing conformers which tend to aggregate and eventually form toxic plaques in brain and other tissue. See Bucciantini, M., et al. (2002) *Inherent Toxicity of Aggregates Implies a Common Mechanism for Protein Misfolding Diseases*. Nature 416:507-511.

These "folding diseases" can be hard to diagnose since the disease symptoms may be latent where the aggre-

1 gates are slowly building up over time and go through
2 stages of increased aggregation leading to fibril formation
3 and eventual plaque deposition leading to impairment of
4 cellular viability. Such misfolding of peptides and aggre-
5 gate formation is believed to play a key role in Alzhei-
6 mer's disease where beta-amyloid protein (or A beta, a 39-
7 42 residue peptide) forms fibrillar deposits upon a con-
8 former change; Huntington's disease where insoluble protein
9 aggregates are formed by expansion of poly-glutamine tracts
10 in the N-terminus of huntingtin (Htt), an antiapoptotic
11 neuronal protein; and noninfectious cancers such as in
12 cases where tumor-associated cell surface NADH oxidase
13 (tNOX) has prion-like properties such as proteinase^R, abil-
14 ity to form amyloid filaments and the ability to convert
15 the normal NOX protein into tNOX. See Kelker, et al.
16 *Biochemistry* (2001) 40:7351-7354. for more information on
17 tNOX.

18 The present invention, however, is not limited to the
19 detection of proteins or peptides in folding-disease or
20 infectious samples. It also includes detection of protein-
21 aceous particles such as prions. Prions are small protein-
22 aceous particles with no nucleic acids, thus are resistant
23 to most nucleic-acid modifying procedures and proteases.
24 The normal prion (PrP) protein is a cell-surface metallo-
25 glycoprotein that is mostly an alpha-helix and loop struc-
26 ture as shown in Fig. 8, and is usually expressed in the
27 central nervous and lymph systems. It's proposed function
28 is that of an antioxidant and cellular homeostasis.

29 The abnormal form of the PrP, however, is a conformer
30 which is resistant to proteases and is predominantly beta-
31 sheet in its secondary structure as shown in Fig. 9. It is
32 believed that this conformational change in secondary

1 structure is what leads to the aggregate and eventual
2 neurotoxic plaque deposition in the prion-disease process.

3 The abnormal prion are infectious particles that play
4 key roles in the transmission of several diseases such as
5 Creutzfeldt-Jakob syndrome, chronic wasting disease (CWD),
6 nvCJD, transmissible spongiform encephalopathy (TSE), Mad
7 Cow disease (BSE) and scrapie a neurological disorder in
8 sheep and goats¹.

9 Diseases caused by prions can be hard to diagnose
10 since the disease may be latent where the infection is
11 dormant, or may even be subclinical where abnormal prion is
12 demonstrable but the disease remains an acute or chronic
13 symptomless infection. Moreover, normal homologues of a
14 prion-associated protein exist in the brains of uninfected
15 organisms, further complicating detection.² Prions associ-
16 ate with a protein referred to as PrP 27-30, a 28 kdalton
17 hydrophobic glycoprotein, that polymerizes (aggregates)
18 into rod-like filaments, plaques of which are found in
19 infected brains. The normal protein homologue differs from
20 prions in that it is readily degradable as opposed to
21 prions which are highly resistant to proteases. Some
22 theorists believe that prions may contain extremely small
23 amounts of highly infectious nucleic acid, undetectable by
24 conventional assay methods.³ As a result, many current
25 techniques used to detect the presence of prion-related
26 infections rely on the gross morphology changes in the
27 brain and immunochemistry techniques that are generally
28 applied only after symptoms have already manifest them-

¹ Clayton Thomas, *Tabor's Cyclopedic Medical Dictionary* (Phil., F.A. Davis Company, 1989), at 1485.

² Ivan Roitt, et al., *Immunology* (Mosby-Year Book Europe Limited, 1993), at 15.1.

³ Benjamin Lewin, *Genes IV* (Oxford Univ. Press, New York, 1990), at 108.

1 selves. Many of the current detection methods rely on
2 antibody-based assays or affinity chromatography using
3 brain tissue from dead animals and in some cases capillary
4 immunoelectrophoresis using blood samples.

5
6 The following is an evaluation of current detection meth-
7 ods.

8
9 o *Brain Tissue Sampling.* Cross-sections of brain can be
10 used to examine and monitor gross morphology changes
11 indicative of disease states such as the appearance of
12 spongiform in the brain, in addition to immunohisto-
13 chemistry techniques such as antibody-based assays or
14 affinity chromatography which can detect disease-spe-
15 cific prion deposits. These techniques are used for a
16 conclusive bovine spongiform encephalopathy (BSE)
17 diagnosis after slaughter of animals displaying clini-
18 cal symptoms. Drawbacks of tissue sampling include
19 belated detection that is possible only after symptoms
20 appear, necessary slaughter of affected animals, and
21 results that takes days to weeks to complete.

22
23 o *Prionic-Check* also requires liquified-brain tissue for
24 use with a novel antibody under the Western Blot tech-
25 nique. This test is as reliable as the immuno-
26 chemistry technique and is more rapid, yielding re-
27 sults in six to seven hours, but shares the drawbacks
28 of the six-month lag time between PrP^s accumulation
29 (responsible for the gross morphology changes) in the
30 brain and the display of clinical symptoms, along with
31 the need for slaughter of the animal to obtain a sam-
32 ple.

- 1 o *Tonsillar Biopsy Sampling.* Though quite accurate, it
2 requires surgical intervention and the requisite days
3 to weeks to obtain results.
- 4
- 5 o *Body Fluids: Blood and Cerebrospinal Sampling.* As in
6 the above detection methods, results are not immediate
7
- 8 o *Electrospray ionization mass spectrometry (ESI-MS),*
9 *nuclear magnetic resonance NMR, circular dichroism*
10 *(CD) and other non-amplified structural techniques.*
11 All of these techniques require a large amount of
12 infectious sample, and have the disadvantage of re-
13 quiring off-site testing or a large financial invest-
14 ment in equipment.
- 15

16 The following is a survey of currently approved and
17 certified European Union (EU) prion-detection tests.

- 18
- 19 o *Prionics -in Switzerland.* The test involves Western
20 blot of monoclonal antibodies (MABs) to detect PrP in
21 brain tissue from dead animals in seven to eight
22 hours.
- 23
- 24 o *Enfer Scientific -in Ireland.* The test involves
25 ELISA-based testing on spinal cord tissue from dead
26 animals in under four hours.
- 27
- 28 o *CEA -in France.* The test involves a sandwich
29 immunoassay using two monoclonals on brain tissue
30 collected after death in under twenty-four hours.
- 31

32 The EU Commission's evaluation protocol has sensitiv-
33 ity, specificity and detection limits and titre. The

1 sensitivity of a test is the proportion of infected refer-
2 ence animals that test positive in the assay. It previ-
3 ously used 300 samples from individual animals to assess
4 this element. The specificity of a test is the proportion
5 of uninfected reference animals that test negative in the
6 assay. Previously used 1,000 samples from individual
7 animals for this purpose. In order to test detection
8 limits, various dilutions ranging from 10^0 to 10^{-5} of posi-
9 tive brain homogenate were used. A table showing an evalu-
10 ation of EU test results is shown in Fig. 12. Even with
11 high degrees of sensitivity and specificity, however, the
12 fact remains that these tests must be performed post-mortem
13 and require working with large amounts of highly infectious
14 biohazard materials.

15
16 The Center for Disease Control (CDC) classifies prions
17 as Risk Group 2 agents requiring Biosafety Level 2 (BSL2)
18 containment. As a result many of the above operations are
19 carried out under BSL2 physical containment with elevated
20 safety practices more typical of a BSL3 lab. Prions can be
21 inactivated by fresh household bleach, 1 molar NaOH, 4
22 molar guanidine reagents, or phenol followed by 4.5 hours
23 of autoclaving at 132°C . Procedures involving brain tissue
24 from human patients with neurological degenerative disor-
25 ders pose special challenges and should be handled with the
26 same precautions as HIV+ human tissue. Thus, working with
27 large amounts of such biohazardous materials can be an
28 obstacle to quick and simple testing of mass quantities or
29 assembly-line samples as well as cumbersome even for small
30 applications.

31
32 In addition to working with relatively large amounts
33 of biohazardous materials and taking several hours to weeks

1 for detection, many of the prior art methods have the added
2 difficulty that they are performed post mortem.

3
4 As can now be seen, the related art remains subject to
5 significant problems, and the efforts outlined above —
6 although praiseworthy — have left room for considerable
7 refinement. The present invention introduces such refine-
8 ment.

9
10
11
12
13 SUMMARY OF THE DISCLOSURE

14
15 The present invention is based on the interaction
16 between low concentration levels of abnormal proteinaceous
17 particles and a peptide fragment or probe to induce trans-
18 formation and propagation of the probe bound to the abnor-
19 mal proteinaceous particles initially present within a test
20 sample. Thus, in a preferred embodiment, infectious levels
21 of a test sample can be propagated even from low concentra-
22 tions.

23
24 The present invention uses catalytic propagation to
25 exploit conformational changes in proteins associated with
26 a particular disease process, such as transmissible spongi-
27 form encephalopathy (TSE). Catalytic propagation basically
28 amplifies the number of existing protein fragments causing
29 aggregates to form. The aggregates of conformationally
30 changed protein fragments are then easily detected using
31 common analytical techniques.

32 As a result, the present invention allows testing to
33 be done using rapid and cost-effective analytical tech-

1 niques, even on, heretofore difficult to detect, small
2 sample sizes and is widely applicable to tissues and body
3 fluids other than those found in brain. Results of the
4 present invention can easily and immediately interpreted
5 using familiar analytical instrumentation. Additionally,
6 the present invention can amplify a weak signal, thus can
7 be successfully applied to small or weak samples such as
8 those associated with body fluids; thereby opening the door
9 to analysis of tissues and fluids for the elusive diseases
10 discussed above. Moreover, this allows the method to be
11 relatively noninvasive in that it does not need to be
12 performed post-mortem; and because it does not need to be
13 performed post-mortem it can be applied to presymptomatic-
14 ally.

15
16 The foregoing may be a description or definition of
17 the first facet or aspect of the present invention in its
18 broadest or most general terms. Even in such general or
19 broad form, however, as can now be seen the first aspect of
20 the invention resolves the previously outlined problems of
21 the prior art.

22
23 Because the present invention allows detection using
24 samples with very low levels of infectious agents and
25 involves amplifying a peptide probe as opposed to a whole
26 potentially infectious protein, many of the previous
27 biohazard-handling concerns are reduced.

28
29 Now turning to another of the independent facets or
30 aspects of the invention: in preferred embodiments of this
31 facet, the peptide probes are designed for the detection of
32 a desired sequence and so have adaptable levels of selec-
33 tivity and specificity built into the method. Also, in-

1 intrinsic optical fluors such as pyrene can be designed into
2 the peptide probe allowing simple, single step optical
3 detection of the abnormal proteinaceous particles.

4
5 All of the foregoing operational principles and
6 advantages of the present invention will be more fully
7 appreciated upon consideration of the following detailed
8 description, with reference to the appended drawings, of
9 which:

10
11
12
13 BRIEF DESCRIPTION OF THE DRAWINGS

14
15 Fig. 1 is a pictorial representation of conformers of
16 transmissible spongiform encephalopathies (TSE) and probes
17 in the form of labeled peptides and labeled dendrimers;

18 Fig. 2 is a pictorial representation of TSE protein
19 detection schema;

20 Fig. 3 is a graph showing the conformational changes
21 associated with a poly-L-lysine test peptide using circular
22 dichroism;

23 Fig. 4 is a graph comparing the circular dichroism
24 results of the poly-L-lysine test peptide at different
25 temperatures and pH;

26 Fig. 5 is a table comparing the circular dichroism
27 results of the poly-L-lysine test peptide at different
28 temperatures and pH;

29 Fig. 6 is a graph of data for fluorescence resonance
30 energy transfer (FRET) experiments for proximal and distal
31 locations in an α -helical bundle structure undergoing
32 conformational change;

1 Fig. 7 is a graph of the driving force necessary to
2 overcome the energy difference between two different

3 Fig. 8 is a structural diagram of a normal PcP pro-
4 tein, a cell-surface metallo-glycoprotein that is expressed
5 in the central nervous and lymphatic systems, and that is
6 characterized as having mostly an alpha-helix and loop
7 structure;

8 Fig. 9 is a structural diagram of the PcP protein that
9 has shifted to a predominately beta structure in which it
10 is likely for form aggregates and neurotoxic fibrils even-
11 tually leading to plaque deposition;

12 Fig. 10 is a pictorial representation of amplification
13 of signal and propagation of conformational change without
14 increased aggregation by the addition of dendrimers of the
15 invention to a test sample;

16 Fig. 11 is a structural diagram of proteins used in
17 the current prior art prion-diagnostic market; wherein
18 Fig. 11a on the left shows the PrPsens protein molecule and
19 Fig. 11b on the right shows a PrPres protein molecule;

20 Fig. 12 is a table evaluating the current prior art in
21 European Union certified prion-diagnostic tests

22 Fig. 13 is a comparison showing selected PrP sequences
23 among six different species;

24 Fig. 14 shows peptide sequences for the synthetic
25 peptide probes Seq. 19 and Seq. 14 of this invention;

26 Fig. 15 is a graph of fluorescence detection experi-
27 mental results showing the effects of peptide concentra-
28 tion;

29 Fig. 16 is a graph of fluorescence detection experi-
30 mental results showing the effects of peptide concentration
31 likely showing excimer emission at approximately 460 nano-
32 meters (nm);

1 Fig. 17 is a graph of fluorescence detection experi-
2 mental results showing pyrene's excitation of fluorescence;

3 Fig. 18 is a graph of fluorescence detection experi-
4 mental results showing pyrene's excitation spectra for
5 fluorescence at 398 and approximately 460 nm;

6 Fig. 19 is a graph comparing the circular dichroism
7 results of several peptides ranging in concentration from
8 20 to 100 milli Molar (mM) under varying buffer conditions;

9 Fig. 20 is a graph comparing the circular dichroism
10 results of several peptides including the synthetic pep-
11 tides of Seq. 19 and Seq. 14 under varying buffer condi-
12 tions;

13 Fig. 21 shows experimental results of the conformatio-
14 nal lability of the synthetic peptides. Fig. 21a on the
15 left shows that Seq. 14 assumes a beta-sheet conformer
16 while the longer analog, Seq. 19 remains coiled. Fig. 21b
17 on the right shows that addition of Seq. 14 to Seq. 19
18 initiates a phase shift to beta-sheet form;

19 Fig. 22 is a conceptual illustration of a comparison
20 of where Seq. 19 and Seq. 14 overlap in structure;

21 Fig. 23 is a graph of experimental results showing
22 that peptides can self-associate;

23 Fig. 24 is a graph of fluorescence data showing the
24 efficiency of excimer formation under low concentrations;

25 Fig. 25 is a graph of fluorescence experimental re-
26 sults showing the effect of nuclei on self-association due
27 to catalytic conformational transition;

28 Fig. 26 contains two graphs of fluorescence experimen-
29 tal results showing the interaction of Seq. 19 and Seq. 14
30 at different ratios; wherein Fig. 26a on the left shows a
31 1:1 mixture and Fig. 26b on the right shows a 100:1 mix-
32 ture;

1 Fig. 27 contains four graphs of fluorescence experi-
2 mental results showing the effect of nuclei on self-associ-
3 ation. Figs. 27a, b, c and d show the results at 24 hours,
4 48 hours, 144 hours and 336 hours, respectively;

5 Fig. 28 is a graph of fluorescence experimental re-
6 sults showing the effect of nuclei on self-association due
7 to catalytic conformational transition at 1 hour in Fig.
8 28a on the left and at 150 hours in Fig. 28b on the right;

9 Fig. 29 shows peptide sequences for a generalized
10 dendrimer structure of this invention;

11 Fig. 30 shows a peptide sequence for a preferred
12 embodiment of a specific dendrimer structure of this inven-
13 tion;

14 Fig. 31 is a conceptual diagram of an experimental
15 device; and

16 Fig. 32 is a system diagram of preferred embodiments
17 of the invention.

18
19
20
21 DETAILED DESCRIPTION
22 OF THE PREFERRED EMBODIMENTS

23
24 It is to be understood that the invention is not
25 limited to the examples described herein. All technical
26 and scientific terms used herein have meanings as commonly
27 understood by one of ordinary skill in the art unless
28 otherwise defined. All publications referred to herein are
29 wholly incorporated by reference to describe methods and
30 materials for implementing aspects of the invention.
31

1 The present invention detects the presence of abnormal
2 proteins and proteinaceous particles based on a method that
3 utilizes catalytic propagation. Upon interaction of a
4 sample, containing abnormal proteins or proteinaceous
5 particles, with a peptide probe of the invention, the
6 peptide probe undergoes conformational changes resulting in
7 the formation of aggregates. The addition of the abnormal
8 proteins and proteinaceous particles catalyzes the forma-
9 tion of the aggregates and causes further propagation of
10 this conformational transition. The resulting aggregates
11 are then easily detected using common analytical instrumen-
12 tation and techniques.

13
14 The abnormal proteins and proteinaceous particles on
15 which the invention focuses are proteins, protein based
16 chemical structures such as prions and protein subunits
17 such as peptides that are capable of conformational changes
18 that lead to the formation of aggregates and ultimately to
19 disease states.

20 These proteins and proteinaceous particles form aggre-
21 gates by shifting from a monomeric to a multimeric state.
22 The shift from one distinct state to the other requires a
23 driving force that is commensurate with the energetic
24 difference between the two conformational states as shown
25 in Fig. 7.

26 A preferred example of such proteinaceous particles is
27 that of a prion protein. Prions can exist in one of two
28 distinct conformations characterized by having a secondary
29 protein structure that is either predominately alpha-heli-
30 cal or predominately beta-sheet; where the predominately
31 beta-sheet conformation has a much higher preference to
32 exist in a multimeric state. As a result, predominately

1 beta-sheet (or beta rich) secondary structure is more
2 typical of abnormally folded or disease-causing proteina-
3 ceous particles since their preference to aggregate is
4 likely to be disruptive in an in vivo environment.

5 Fig. 1 shows illustrations of both the alpha-helical
6 monomer 10 and the beta-sheet dimer 12 forms of a TSE
7 conformer (or alternative secondary structure). Research
8 has shown that the normal wild-type (wt) form of prion
9 protein (PrP^C) prefers a monomeric state, while the abnor-
10 mal, disease-causing form (PrP^{Sc}) more readily takes on a
11 multimeric state.⁴

12 This distinction between the secondary structure of
13 the normal form of prion protein and the abnormal form as
14 well as its propensity to cause aggregation is exploited in
15 the present invention to allow detection of the abnormal
16 form even in samples with very low levels of infectious
17 abnormal protein.

18 The mechanism of the invention is shown in a schematic
19 in Fig. 2. The top row of the schematic shows an example
20 of an unknown sample of TSE protein represented as contain-
21 ing beta-sheets 12. The beta-sheets are then disaggregated
22 by subjecting the sample to commonly known disaggregation
23 methods such as sonication. This is followed by the addi-
24 tion of labeled peptide probes 14 which are allowed to bind
25 to the sample 12. Presence of the beta-sheet conformation
26 in the sample 12 induces the peptide probes to also shift
27 to beta-sheet formation 16. In this manner the transition
28 to beta-sheet is propagated among the peptide probes 14
29 thereby causing new aggregates 18 to form. The resulting
30 transition to a predominately beta-sheet form and amplified

⁴ Fred E. Cohen, et al., *Pathologic Conformations of Prion Proteins* (Annu. Rev. Biochem. 1998) 67: 793-819.

1 aggregate formation can then easily be detected using
2 common analytical techniques such as light scattering and
3 circular dichroism (CD); and in a particularly preferred
4 embodiment where the peptide probe is fluorescent labeled,
5 fluorescence detection instrumentation can also be used.

6 The bottom row of Fig. 2 shows an alternative example
7 in which the unknown sample of TSE protein is represented
8 in its normal alpha-helical form 10. For consistency, the
9 sample is subjected to the same disaggregation process
10 described above. Upon addition of the labeled peptide
11 probes 14, neither a transition to beta-sheet form nor
12 binding to the unknown samples occurs. As a result, there
13 is no aggregate fluorescence signal in the case of a la-
14 beled peptide probe as well as no detection of aggregate
15 formation by other analytical tools. Based on this sche-
16 matic, unknown samples can be tested for the presence or
17 absence of such abnormal protein conformations or se-
18 quences.

19
20 A preferred embodiment of the invention involves the
21 following basic procedures. Peptide probes 14 are selected
22 in order to be added to an unknown or test sample 20 at a
23 later stage in the process. The peptide probes 14 are
24 preferably proteins or peptide sequences that have second-
25 ary structures of predominately alpha-helix or random coil.
26 In a particularly preferred embodiment, the peptide probes
27 14 are peptide fragments consisting of a helix-loop-helix
28 structure as found in lysine. In another particularly
29 preferred embodiment, the peptide probes can be made of a
30 peptide sequence chosen from wild-type (wt) TSE, from a
31 desired species-specific TSE peptide sequence, or even from
32 a selectively mutated TSE sequence that has been mutated in

1 such a manner as to render it destabilized and noninfec-
2 tious. Additionally, extrinsic fluors such as pyrene can
3 be added or designed into the peptide probe to allow detec-
4 tion of anticipated conformational changes using common
5 fluorescence detection techniques.

6 Once a peptide probe 14 is selected, it is added to a
7 test sample 20. Prior to the addition of the peptide probe
8 14, however, it is preferred to have the sample 20 sub-
9 jected to disaggregation techniques commonly known in the
10 art, such as sonication. The disaggregation step allows
11 any potentially aggregated sample material 20 to break
12 apart so that these disaggregated sample materials 22 are
13 more free to recombine with the newly introduced peptide
14 probes 14; thereby facilitating the anticipated catalytic
15 propagation.

16 After the test sample 20 or disaggregated test sample
17 22 is allowed to interact with the peptide probes 14. The
18 resulting mixture is then subjected to analytical methods
19 commonly known in the art for the detection of aggregates
20 and to fluorescence measurements in cases where fluorescent
21 peptide probes 14 are used.

22 Unknown or test samples 20 containing any dominant
23 beta-sheet formation characteristic of abnormally folded or
24 disease-causing proteins results in an increase in beta-
25 sheet formation and consequently aggregate formation in the
26 final mixture containing both the test sample 20 and the
27 peptide probes 14. Conversely, unknown or test samples 20
28 which lack a predominantly beta-sheet secondary structure
29 will neither catalyze a transition to beta-sheet structure
30 16 nor will propagate the formation of aggregates 18.
31

1 One of ordinary skill in the art can appreciate that
2 the
3 means by which the initial conformational change can be
4 triggered in the test samples 20 can be varied as described
5 in the following examples. The binding of a metal ligand
6 could direct a change in the protein scaffolding and favor
7 aggregation. The expression or cleavage of different pep-
8 tide sequences can promote advanced aggregation leading to
9 fibril and plaque formation. Genetic point mutations can
10 also alter the relative energy levels required of the two
11 distinct conformations, resulting in midpoint shifts in
12 structural transitions. Furthermore, an increase in con-
13 centration levels could be sufficient to favor the
14 conformational transition. Regardless of the initial
15 trigger mechanism, however, the disease process in many of
16 the abnormal protein conformations such as in prion-related
17 diseases always involves the catalytic propagation of the
18 abnormal conformation, resulting in transformation of the
19 previously normal protein.

20
21 One of ordinary skill in the art can also appreciate
22 that there are many common protein aggregate detection
23 techniques many of which are based on optical measurements.
24 These optical detection techniques include, but are not
25 limited to, light scattering, or hydrophobicity detection
26 using extrinsic fluors such as 1-anilino-8-napthalene
27 sulfonate (ANS) or Congo Red stain, fluorescence proximity
28 probes on the peptide fragments, including fluorescence
29 resonance energy transfer (FRET) & quenching of intrinsic
30 tryptophan fluorescence through either conformational
31 change of monomer or binding at interface in alpha-beta
32 heterodimer; the N-terminal loop region is particularly

1 interesting in this regard selective binding to target
2 protein, circular dichroism (CD) monitoring of actual
3 conformation, nuclear magnetic resonance (NMR). Other
4 detection techniques include equilibrium ultracentrifuga-
5 tion or size-exclusion chromatography at the aggregation
6 stage as well as other structural techniques. Examples and
7 explanations of these methods can be found in Freifelder,
8 David. *Physical Biochemistry: Applications to Biochemistry*
9 *and Molecular Biology*, (W. H. Freeman Press, New York, 2nd
10 ed. 1982). and in Copeland, Robert. *Analytical Methods for*
11 *Proteins*, (American Chemical Society Short Courses 1994).
12 both of which are wholly incorporated herein as prior art.
13 Many of these enumerated optical and structural methods are
14 rapid, cost-effective and accurate.

15
16 Experiments were performed using model systems to show
17 the conformational changes involved in the transition from
18 a predominately alpha-helix to a beta-rich form. The model
19 systems chosen used readily available, nonneurotoxic poly-
20 amino acids such as polylysine and polyglutamine. The
21 polyamino acids were chosen because of their availability
22 and more importantly because they are safe to handle thus
23 eliminating the need for special handling or donning cum-
24 bersome extra protective gear.

25 Fig. 3 shows a circular dichroism graph of experimen-
26 tation with poly-L-lysine 20 micro Molar (μM) 52,000 molec-
27 ular weight (MW) as a peptide probe. The resulting graphs
28 show:

- 29
30 • Sample 24 which was maintained at pH7, 25°C result-
31 ing in a minimum at approximately 205 nanometers (nm)
32 indicating random coil structure.

1 • Sample 26 which was maintained at pH11, 50°C result-
2 ing in a minimum at approximately 216 nanometers (nm)
3 indicating beta-sheet structure.

4
5 • Sample 28 which was a 1:1 combination of samples
6 maintained at pH7, 25°C and at pH11, 50°C resulting in
7 a minimum at approximately 216 nanometers (nm) indi-
8 cating beta-sheet structure.

9
10 • Sample 30 which was a 1:1 combination of samples
11 maintained at pH7, 50°C and at pH11, 50°C resulting in
12 a minimum at approximately 216 nanometers (nm) indi-
13 cating beta-sheet structure.

14
15 Fig. 4 shows an absorbance graph of experimentation
16 with poly-L-lysine 70 micromolar (μM) 52,000 molecular
17 weight (MW) as a peptide probe. The resulting graphs show:

18
19 • Sample 32 which was maintained at pH 11, 25°C re-
20 sulting in a plateau at approximately 0.12 indicating
21 predominately alpha-helical structure.

22
23 • Sample 34 which was maintained at pH7, 50°C result-
24 ing in a a plateau at approximately 0.22 indicating
25 random coil structure.

26
27 • Sample 36 which was a 10:1 combination of samples
28 maintained at pH7, 50°C and at pH11, 50°C resulting in
29 a steeper incline from approximately 0.22 to 0.33
30 indicating an accelerated transition from random coil
31 to beta-sheet structure.

32

1 • Sample 38 which was a 10:1 combination of samples
2 maintained at pH7, 25°C and at pH11, 50°C resulting in
3 a gradual incline from approximately 0.22 to 0.26
4 indicating a transition from random coil to beta-sheet
5 structure.

6
7 Fig. 4 shows general circular dichroism results of
8 experimentation with poly-L-lysine at varying temperatures
9 and pH indicating its potential for transitioning from
10 random coil to beta-sheet under the varying environmental
11 conditions. The results indicate that both temperature and
12 pH play an important role in the transition.

13
14 The observations based on all of the modeling experi-
15 mentation described above show that the addition of a
16 relatively small amount of beta-sheet peptide to random
17 coil sample can result in a shift towards a beta-rich
18 conformation and such changes can be accelerated depending
19 on the temperature and pH environment of the samples.

20
21 Fig. 6 shows experimentation results using pyrene as a
22 fluorescent probe in proximal and distal locations in an
23 alpha helical bundle structure undergoing conformational
24 change. The pyrene excimer formation 42 is shown at 480 nm
25 and the spectra for a predominately alpha-helical structure
26 40 is contrasted as well. Those skilled in the art would
27 appreciate that other fluorescent probes such as FITC can
28 also be used.

29
30 A primary objective of this invention also encompasses
31 use of the catalytic propagation of conformational change
32 to directly correlate the measures of abnormal prion pres-

1 ence with levels of infectivity. For this reason we favor
2 implementation of the invention in a manner where there is
3 no increase in resulting infectious products as a result of
4 the propagation. This can be achieved by placing a "break"
5 in the links between the chain of infection, transmission
6 and propagation of the abnormal form. Such a "break" must
7 occur at the transitional stage between the dimer and
8 multimer forms of the aggregate. The physical formation of
9 the multimer form can be blocked by simply impeding the
10 step which leads to its formation. This may be done,
11 preferably by using a large pendant probe or by a neutral
12 "blocker" segment, bearing in mind that probes on linkers
13 or "tethers" are more likely to encounter each other and
14 thus result in amplifying the signal.

15
16 In a particularly preferred embodiment of the inven-
17 tion, the peptide probes 14 function in the manner de-
18 scribed above. The peptide probes act as "nuclei"; wherein
19 once the peptide probe 14 binds to a test sample 20, or a
20 sample known to have beta-rich structure 12, it is con-
21 verted to a peptide probe conformer 16 which has the capac-
22 ity to act as a trigger to bind to another peptide probe 14
23 and continues to induce the same conformational change.
24 Propagation of this reaction can then be controlled by the
25 peptide sequence chosen for the peptide probe 14 and by the
26 experimental conditions. Thus, in situations where infec-
27 tious levels are low and there is a need to amplify any
28 existing abnormal proteinaceous particles in an unknown
29 sample 20, it is preferred that a peptide probe 14 capable
30 of rapid and continuous propagation of the reaction be
31 chosen with which to nucleate the unknown sample 20. On
32 the other hand, in situations where it is desired to corre-

1 late detection of abnormally folded proteinaceous particles
2 with levels of infectivity, it is preferred that peptide
3 probe 14 chosen is one that is less likely to aggregate.

4 When more than one beta units come together, they act
5 as nuclei to attract and stabilize other transient elements
6 of secondary structure. See Stryer, Lubert. *Biochemsitry*.
7 W. H. Freeman Press. (3rd ed. NY 1988) p35. In choosing
8 the peptide probe 14 with which to nucleate this reaction
9 there are several considerations to be made. Associations
10 of peptide can be controlled by the thermodynamics of the
11 solution in which they are in and by the presence of amor-
12 phous nuclei which self-associate, crystalline nuclei which
13 readily aggregate, specific peptide sequences which may
14 aggregate, but may do so under low concentrations which are
15 difficult to measure by conventional means, or larger
16 peptide sequences modeled after known beta-sheet structures
17 or proteins such as a beta-rich prion protein.

18
19 To demonstrate this embodiment of the invention, two
20 peptide sequences were synthesized to be used as peptide
21 probes 14. The peptide sequences were modeled after known
22 prion protein (PrP) sequences shown in Fig. 13. The se-
23 quences in Fig. 13 correspond to binding regions that are
24 very similar among the species shown. Fig. 14 shows the
25 peptide sequences of the two synthesized peptides. The 19-
26 mer sequence referred to as Seq. Id. No. 19 is closely
27 modeled after residues 104 through 122 of the human se-
28 quence. The 14-mer sequence referred to as Seq. Id. No. 14
29 is closely modeled after residues 109 through 122 of the
30 human PrP sequence. The synthetic peptide probes 14 were
31 also prepared with and without pyrene butyric acid as a
32 fluorescence marker.

1 Many experiments were performed to study the proper-
2 ties of the synthetic peptides. Experiments were performed
3 using analytical techniques common in the art such as
4 absorbance, fluorescence under varying excitation and
5 excitation of fluorescence. The peptides were studied at
6 several concentrations ranging from 1 to 100 micro Molar
7 (μM) and under varying buffer concentrations, pH, tempera-
8 tures and ionic strengths.

9 Fig. 15 shows a graph of fluorescence-spectra results
10 at different peptide concentrations. The data were col-
11 lected over times ranging form one hour to one week with no
12 experimental changes observed after twenty-four hours. The
13 resulting graphs show:

14
15 • Sample 46 which was at a concentration of 5 μM with
16 a relative fluorescence peak at approximately 0.1.

17
18 • Sample 48 which was at a concentration of 10 μM
19 with a relative fluorescence peak at approximately
20 0.4.

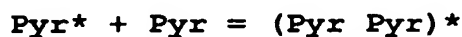
21
22 • Sample .50 which was at a concentration of 150 μM
23 with a relative fluorescence peak at approximately
24 4.7.

25
26 Note: data were also collected for Sample 52 at a high
27 concentration of 800 μM , but is not shown in the figure.

28
29
30 Fig. 16 shows a graph of the fluorescence spectra for
31 samples 46 through 52 normalized to the intensity at 378 nm
32 for the initial scan. It was observed that the spectrum

1 for Sample 52 which contained the highest peptide concen-
2 tration was markedly different leading to the conclusion
3 that there is excimer emission with a maximum at approxi-
4 mately 460 nm.

5
6 Fig. 17 is a graph of experimental results showing
7 pyrene's excitation of fluorescence. The experiments were
8 performed with excitation wavelengths at 365 nm to observe
9 excimer emission at approximately 460 nm. The excitation
10 at 348 nm, however, increases the fluorescence signal by
11 over a hundred times with no other modifications or signal
12 amplification. To confirm that the pyrene conjugate was
13 responsible for both the major 398 nm emission as well as
14 the one at approximately 460 nm, the excitation spectra for
15 fluorescence at 398 nm and at approximately 460 nm were
16 recorded and are shown in Fig. 18. Both the excitation
17 spectra are nearly identical with a 365 nm maximum confirm-
18 ing that emission at approximately 460 nm is associated
19 with the formation of excimers by two pyrene groups as in
20 the following.



23
24 where Pyr is a pyrene molecule and Pyr* is a pyrene in its
25 excited form; the (Pyr_Pyr)* represents the formation of
26 excited dimer. More general information on excimers can be
27 found in Freifelder, David. *Physical Biochemistry: Appli-*
28 *cations to Biochemistry and Molecular Biology*, (W. H.
29 Freeman Press, New York, 2nd ed. 1982), at 559.

30
31 Experiments were also performed to study the stability
32 of the peptides. Fig. 19 shows experimental data obtained

1 from circular dichroism (CD) analysis of the 19-mer under
2 different condition. The CD spectra were recorded for a
3 number of peptide concentrations ranging from 20 to 100 mM.
4 The results show that the 19-mer is largely coiled and
5 exhibits high thermodynamic stability under the experimen-
6 tal conditions tested such as varying pH, ionic strength
7 and temperature. As expected, the addition of organics
8 such as acetonitrile and trifluoroethylene (TFE) encourage
9 the formation of the secondary structure. Fig. 20 shows
10 both the previous results and the results of a similar
11 experiment in which the 19-mer was mixed with its shorter
12 analog, the 14-mer. In this experiment, the 19-mer and 14-
13 mer were combined 100:1 for one hour and assembled under
14 dilute conditions in the micro molar range. Sample curves
15 60 through 64 which correspond to the mixture showed that
16 the mixture of the oligomers significantly differed from
17 the CD spectra of sample curves 52 through 58 which repre-
18 sent the 19-mer alone, indicating strong interactions
19 between the mixed molecules. As a result, the 14-mer
20 triggers conformational changes in a peptide probe 14 made
21 of the 19-mer.

22 In a paper published by Prusiner, et al., CD data show
23 that the Seq. Id. No. 19, 19-mer exhibits coil-like confor-
24 mation, whereas the Seq. Id. No. 14, 14-mer is largely
25 beta-sheet as shown in Fig. 21a for a 3 mM concentration
26 sample from the paper. The 19-mer, however, can be trans-
27 formed from its coil-like conformation to a beta-sheet
28 conformation through interaction with a very small fraction
29 of the 14-mer as shown in Fig. 21b which was tracked over a
30 twenty four hour time period. See Prusiner, et al. *Prion*
31 *protein peptides induce alpha-helix to beta-sheet*

1 conformational transitions. Biochemistry. 34:4186-92 (1995).

2 Fig. 22 shows a conceptual figure of the secondary
3 structure of the two synthetic peptides (where C = coil and
4 H =helix) based on the application of various secondary
5 structure algorithms to the sequences of both of the syn-
6 thetic peptides. The resulting projection, however, does
7 not entirely agree with the CD results. Based on the CD
8 results, the conformations of both synthetic peptides are
9 clearly concentration dependent. Moreover, while the 19-
10 mer exhibits largely a coil conformation that is fairly
11 stable under a wide variety of the experimental conditions
12 tested, the 14-mer exhibits a transition from coil or
13 hairpin to beta-sheet structure depending on its concentra-
14 tion.

15 More experiments were performed to determine if the
16 19-mer could self-associate. Fig. 23 shows a graph of
17 fluorescence results showing that the 19-mer could self-
18 associate with increasing concentration as shown in Sample
19 curve 66 and at low concentrations with pH modifications to
20 give a net neutral charge while using potassium chloride
21 (KCl) to screen the charge as shown in Sample curve 68.
22 The 19-mer can also self-associate at low concentrations
23 with the introduction of some type of nucleating agent, as
24 discussed earlier. Thus, the conditions for self-associa-
25 tion can be optimized to adapt to a desired type of detec-
26 tion.

27 The same samples; Sample curve 66 containing 0.1 M
28 TRIS buffer at pH 6 to 9 and Sample curve 68 containing 0.1
29 M TRIS buffer at pH 10 to 11 in the presence of KCl at 100
30 to 500 mM, are shown again in Fig. 24 to reflect the effi-
31 ciency of excimer formation under low concentrations. The
32 ratio of the fluorescence intensities as measured at 378 nm

1 (I_M) and at 460 nm (I_E) was chosen to monitor the self-
2 association as a function of the peptide concentration at
3 25°C. It was also shown that screening of the electro-
4 static interactions (pI = 10) encouraged self-association
5 at extremely low concentrations on the order of less than
6 10 micro Molar.

7 In order to further study the effect of nuclei on the
8 self-association of the 19-mer, more fluorescence measure-
9 ments were taken of 19-mer in solution nucleating with
10 small amounts of already self-associated 19-mer units. The
11 sample solutions range from concentrations of 200 to 800
12 micro Molar and are described in Fig. 25. The kinetics of
13 association in dilute solutions of 20 micro Molar were also
14 monitored.

15 Fig. 26a shows more fluorescence data of the 19-mer in
16 water 70, acetonitrile 72 and TFE 74 after twenty-four
17 hours. Fig. 26b shows the experimental results for a 100:1
18 combination of the 19-mer and 14-mer in water 76, aceto-
19 nitrile 78 and TFE 80 after twenty-four hours. In both of
20 the graphs in Fig. 26 peptide association was monitored by
21 the appearance of excimer emission at approximately 460 nm.

22 Figs. 27 a, b, c, and d show four fluorescence data
23 graphs taken at 24, 48, 144 and 336 hours, respectively.
24 The measurements were taken to determine the effect of pH,
25 temperature, ionic strength, and organic additives on the
26 kinetics of the peptide associations studied for the 19-mer
27 model peptide. The fluorescence intensities as measured at
28 378 nm for monomeric units and 460 nm for associations were
29 used to characterize the I_E/I_M ratio or self-association of
30 the peptide.

31 Additional fluorescence results are shown in Fig. 28
32 where an insoluble fraction of the peptide was extracted

1 and dissolved in organic solvent containing methanol /etha-
2 nol/ dimethylformamide and then analyzed. Fluorescence
3 detection results of the "insoluble" portion show high
4 levels of peptide association wherein the I_E/I_M ratio equals
5 2. A small aliquot of "insoluble" portion was added to
6 nucleate 20 micro Molar 19-mer peptide solutions which were
7 then analyzed and are reported in the same graph. The
8 results show that the presence of the nucleating fraction
9 significantly increased the efficiency of the peptide
10 association and this can be seen more dramatically in Fig.
11 28b at 150 hours.

12
13 The observations of these experiments led to some of
14 the following conclusions.

15
16 • Fluorescence of pyrene, which is covalently attached
17 to the peptide probe 14 in preferred embodiments,
18 allows monitoring of peptide self-association in this
19 model system. It can also be used as an index of
20 conformational change and especially since at low
21 concentrations, the peptide association is difficult
22 to measure using nonoptical techniques.

23
24 • The fluorescence data shows that self-association of
25 the Seq. Id. No. 19, 19-mer, can be promoted by ad-
26 justing ionic strength or pH.

27
28 • The fluorescence data also shows that the kinetics
29 of the conformational changes can be modulated by
30 controlling solvent parameters and the peptide probe
31 sequence.
32

1 • The kinetics of the self-assembly or association
2 process can be controlled or regulated by the addition
3 of or by preexisting nucleating associated forms.
4 This strongly supports the conclusions that the
5 conformational transitions of the 19-mer can be
6 autocatalytic.

7
8
9 In a particularly preferred embodiment, the peptide
10 probes 14 can be used to detect proteinaceous particles
11 such as in prion-like structures exhibiting coil to beta-
12 sheet transition. According to Prusiner, et al. *Prion*
13 *protein peptides induce alpha-helix to beta-sheet*
14 *conformational transitions. Biochemistry. 34:4186-92*
15 (1995). As a result, synthetic peptide probes such as the
16 Seq. Id. No. 19, 19-mer should be conformationally sensi-
17 tive to the presence of prion-like substances that undergo
18 this conformational shift. Moreover, because an intrinsic
19 optical reporter, such as pyrene can be added to the pep-
20 tide probe, this embodiment of the invention has the added
21 advantage of being able to detect such prion-like sub-
22 stances in test samples 20 such as blood, lymph, CSF and
23 even tissues other than brain homogenate that typically
24 contain very low levels of abnormal prion substances that
25 are otherwise too difficult to detect. The intrinsic
26 optical reporter allows optical (fluorescence) measurements
27 to be taken of the peptide probe associates that form upon
28 interaction with nucleating samples such as an abnormal
29 prion.

30
31 In another particularly preferred embodiment of the
32 invention, the peptide probes 14 are synthesized based on

1 the structure of a dendrimer; dendrimers being synthesized
2 three-dimensional highly branched macromolecules. The
3 advantages of using a dendrimer probe 15 are multifold.
4 Dendrimers should increase the speed of the assay kinetics
5 thereby relaying quicker test results. This can be espe-
6 cially advantageous in assembly line applications of the
7 invention where products or specimens in mass quantities
8 can be quickly tested for the presence of abnormal
9 proteinaceous particles. This embodiment is also extremely
10 beneficial in applications where quick decisions must be
11 based on the detection results. This embodiment is also
12 advantageous for use in these applications as well as
13 others since the highly branched structure of the dendrimer
14 prevents amplification of abnormal proteinaceous particles
15 or aggregates. By preventing such amplification of the
16 abnormal particles, it becomes very simple to correlate the
17 detection results with the level of abnormal aggregates
18 existing in a test sample 20. Furthermore, it is also safe
19 to handle since the synthetic probe itself is nonneurotoxic
20 and amplifies signal without amplification of any highly
21 infectious particles that may be preexisting in a test
22 sample 20. Thus, it eliminates the need for extra precau-
23 tions or sterilization in many of the steps of the assay
24 method.

25 A generalized dendrimer 15 structure is shown in Fig.
26 29 and is referred to as Seq. Id. No. 20. In a particu-
27 larly preferred embodiment of the invention, a specific
28 dendrimer structure was designed and synthesized, referred
29 to as Seq. Id. No. 22 and is shown in Fig. 30.

30 In Fig. 30, the specific dendrimer structure is basi-
31 cally a loop-turn-loop structure as illustrated by Fig.
32 30a. In Fig. 30b, it is shown that the sequence is modeled

1 after the human PrP sequence shown in Fig. 14 in residues
2 126 through 104 plus 109 through 126. This structure shows
3 the region on the right 74 as an inverted form of the PrP
4 sequence. This was done to take advantage of the five
5 aminoacids which naturally form a loop in order to place
6 hydrophobic pyrene in a corresponding hydrophobic region.
7 Also the valine-valine fragment is essential to beta-sheet
8 formation and so is retained in the sequence. In the
9 figure, green denotes possible mouse variants. The
10 amyloidogenic palindrome region 70 may be changed to SS or
11 SSS/AAA. The central region 72 is a loop sequence with
12 steric constraints, thus it is possible to add tryptophan
13 for steric and fluorescence considerations.

14 Modifications of the aminoacid sequence such as one or
15 more deletions or insertions are possible as alluded to
16 above, provided that the dendrimer retains its branched
17 loop-turn-loop structure as well as aminoacids essential to
18 beta-sheet formation, and preferably contains an optical
19 reporter.

20 Fig. 10 shows a schematic diagram of how the dendrimer
21 probes 15 amplify signal and propagate conformational
22 change without aggregation and without increasing the
23 biohazard or infectious nature of an abnormal protein or
24 prion test sample 12. The figure shows that once the
25 dendrimer probes 15 come into contact with the abnormal
26 sample 12, the dendrimer probe 15 undergoes the
27 conformational shift to a predominately beta-sheet struc-
28 ture 17. The newly formed beta-rich dendrimer probe 17
29 nucleates other dendrimer probes 15 to make the same tran-
30 sition. By doing so, any optical signal associated with
31 the dendrimer probe 15 is amplified as more probes 15 shift
32 to the beta-rich state 17.

1 It is important to note that the minimal detectable
2 concentration of pyrene only provides a number for the
3 peptide probe 14 concentration that can be worked with; but
4 the detection limit of the assay is not dependent on it
5 because it is the resultant of the fluorescent ensemble
6 that is being observed. In other words, the real measure-
7 ment of interest and the rate limiting step in the analysis
8 is the amount of abnormal e. g. prion protein that need to
9 be present in the sample 20 to initiate a conformer change
10 in the peptide probe 14. Immunoassays are typically sensi-
11 tive in the picomolar range. Nevertheless, once the con-
12 former change is initiated in a single peptide probe 14,
13 the catalytic propagation of its beta-rich structure allows
14 detection in samples previously considered to have abnormal
15 particles 12 at concentrations too low to detect.

16
17 Due to its ability to safely, quickly and noninvasive-
18 ly detect abnormal proteinaceous particles such as misfol-
19 ded proteins, prions, aggregates and fibrils that may lead
20 to toxic plaque formations, the method of this invention is
21 widely applicable to many industries. By example, some of
22 those industries include the diagnostics markets in animal
23 health and human health, the food industry, pharmaceuticals,
24 especially for screening animal by-products,
25 transplant/transfusion and vaccine supplies, research and
26 development in such areas as chemotherapies for TSE's, as
27 well as national security in the area of biosensors for
28 biowarfare agents.

29 Accordingly, in yet another preferred embodiment of
30 the invention, the methods discussed herein can be applied
31 for use with a simple detection instrument such as the one
32 shown in Fig. 31. The device shown in Fig. 31 is a simple

1 optical device that includes a light source 80 shown in
2 blue e. g. lamp or laser; a T-format sample cell 82 shown
3 in grey; and a photomultiplier tube 84 shown in pink. In
4 certain applications it may be desirable to have the method
5 distributed as an assay that includes such a simple device.
6

7 Accordingly, the present invention is not limited to
8 the specific embodiments illustrated herein. Those skilled
9 in the art will recognize, or be able to ascertain that the
10 embodiments identified herein and equivalents thereof
11 require no more than routine experimentation, all of which
12 are intended to be encompassed by claims.

13 Furthermore, it will be understood that the
14 foregoing disclosure is intended to be merely exemplary,
15 and not to limit the scope of the invention -- which is to
16 be determined by reference to the appended claims.

WHAT IS CLAIMED IS:

1 1. A method for rapid preclinical detection of infectious
2 conformationally altered proteins; said method comprising:
3 obtaining a test specimen;
4 adding a propagation catalyst to the specimen;
5 allowing the catalyst and the specimen to interact
6 forming a mixture; and
7 observing any increase in beta-sheet formation in the
8 mixture.

1 2. The method of claim 1, wherein:
2 said obtaining step does not include physically sacri-
3 ficing a subject from which the test specimen is obtained.

1 3. The method of claim 1, wherein:
2 said obtaining step is noninvasive in that it encom-
3 passes drawing body fluids but does not encompass biopsy of
4 tissues or organs.

1 4. The method of claim 1, wherein:
2 said propagation catalyst is an agent which undergoes
3 a conformational shift toward beta-sheet formation upon
4 contact with a proteinaceous particle.

1 5. The method of claim 4, wherein:
2 said propagation catalyst is an optical labeled pep-
3 tide.

1 6. The method of claim 4, wherein:
2 said peptide is a peptide having the amino acid se-
3 quence of Seq. Id. No. 19.

1 7. The method of claim 1, wherein:
2 said propagation catalyst is a dendrimer.

1 8. The method of claim 7, wherein:
2 said dendrimer is a dendrimer having the amino acid
3 sequence of Seq. Id. No. 20.

1 9. The method of claim 7, wherein:
2 said dendrimer is a dendrimer having the amino acid
3 sequence of Seq. Id. No. 22.

1 10. The method of claim 4, wherein:
2 said proteinaceous particle is a predominately beta-
3 sheet structure.

1 11. The method of claim 4, wherein:
2 said proteinaceous particle is a PrP^{sc} particle.

1 12. The method of claim 1, wherein:

2 addition of said propagation catalyst to a test speci-
3 men containing selected abnormal proteinaceous particles
4 increases beta-sheet formation of the propagation catalyst.

1 13. The method of claim 1, wherein:

2 addition of said propagation catalyst to a test speci-
3 men containing PrP^{Sc} increases beta-sheet formation of the
4 propagation catalyst.

1 14. The method of claim 1, wherein:

2 said propagation catalyst is an abnormal proteinaceous
3 particle (PrP^{Sc}).

1 15. The method of claim 10, wherein:

2 addition of said propagation catalyst to a test speci-
3 men containing proteinaceous particles of substantially
4 only a PrP^{Sc} type cause an increase in beta-sheet formation
5 of the mixture.

1 16. The method of claim 1, further comprising:

2 designation of a test subject requiring therapeutic
3 treatment based on the detection of infectiously
4 conformationally altered protein in the sample taken from
5 such test subject.

1 17. The method of claim 1, wherein:
2 the test subject is a human being.

1 18. The method of claim 1, wherein the steps of obtaining
2 and observing involve receiving and monitoring of products
3 from the group consisting of:
4 health research, pharmaceuticals, food industry and
5 biosensors for national security.

1 19. The method of claim 1, method of claim 1, wherein the
2 steps of observing involve monitoring of products from the
3 group consisting of:
4 animal by-products, chemotherapies, transplant, trans-
5 fusion and vaccine supplies.

6
7
8 20. A method for using a device for rapid preclinical
9 detection of infectious conformationally altered proteins,
10 wherein said device comprises:
11 a light source;
12 a flow cell; and
13 a photomultiplier.

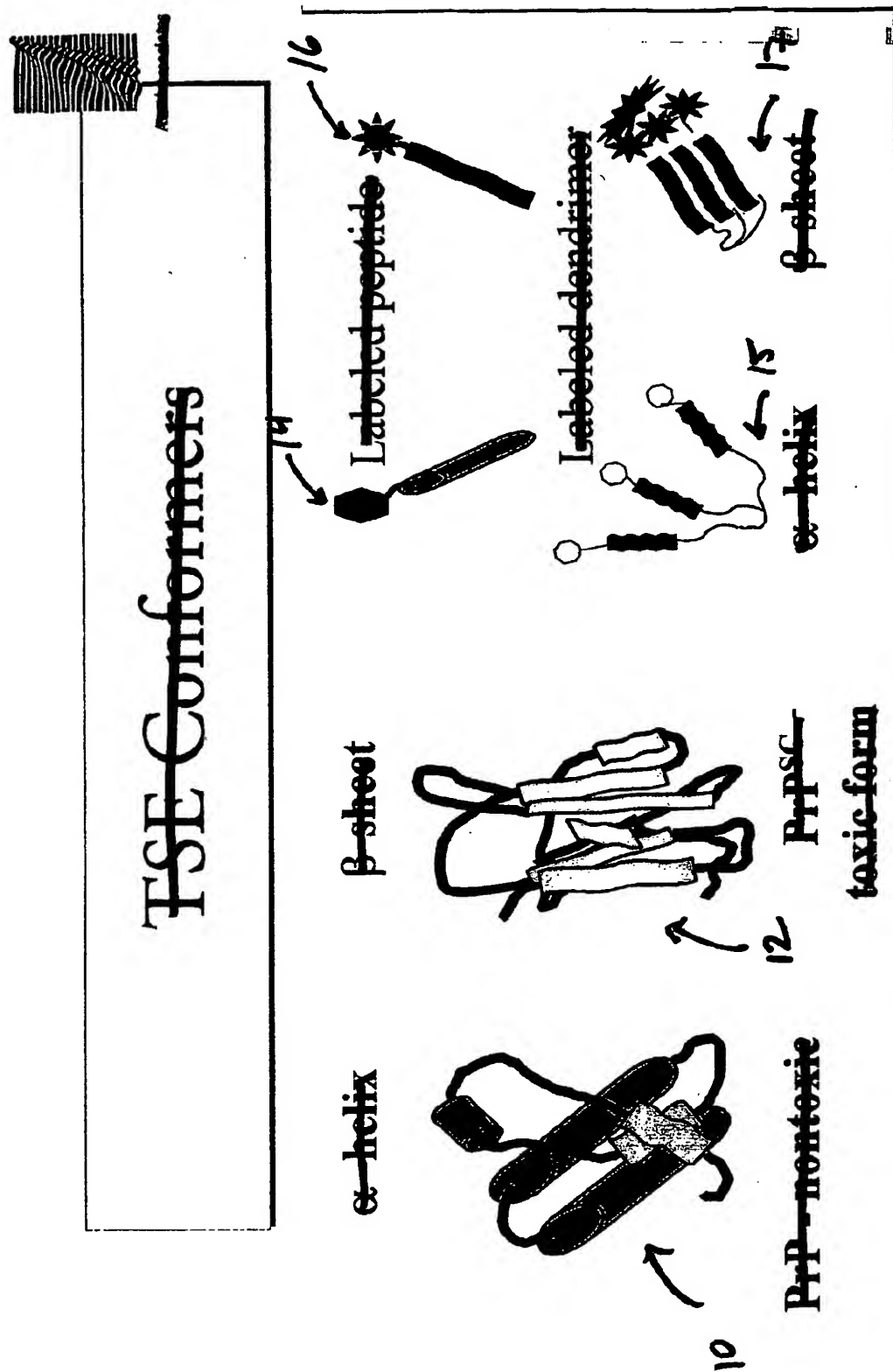
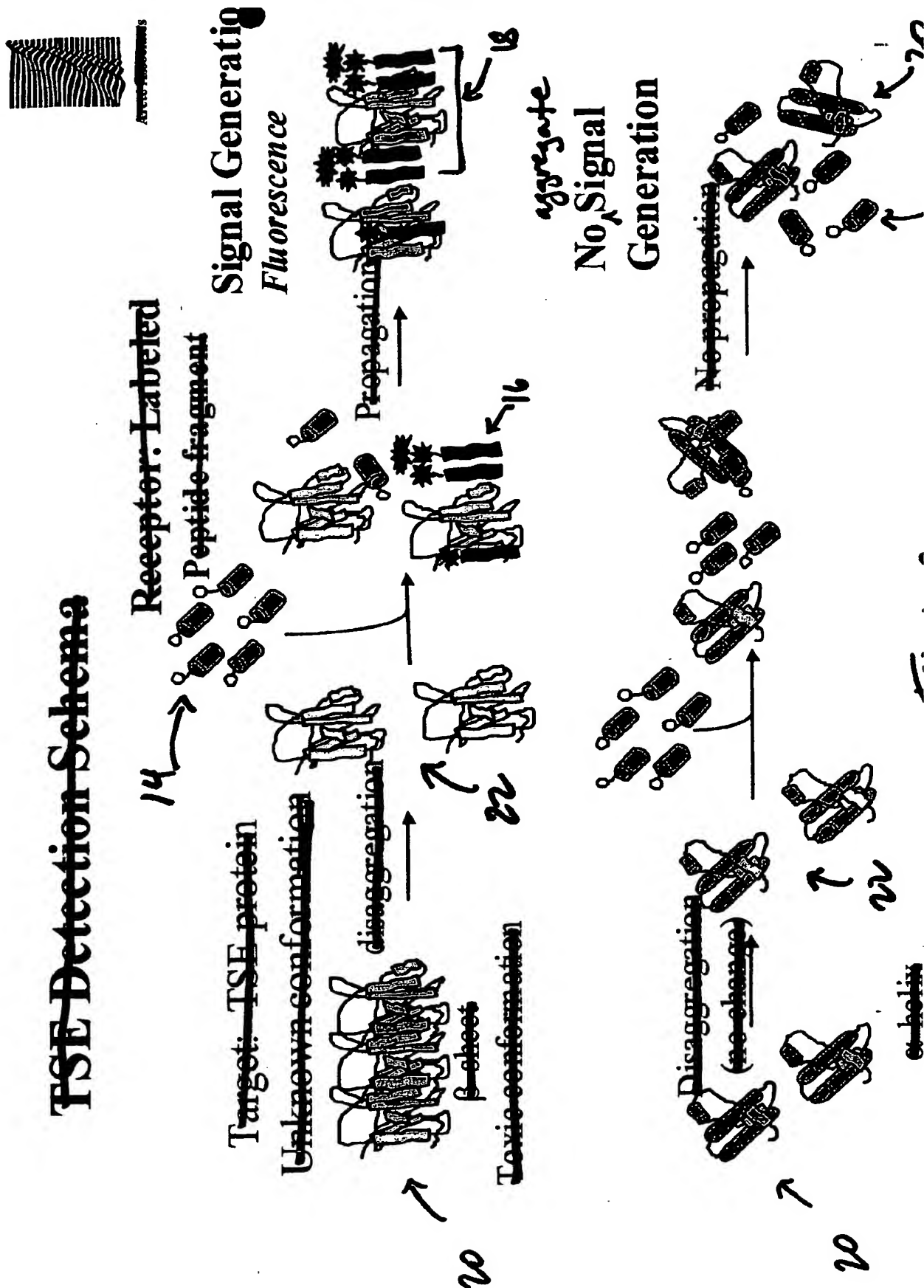


Figure 1

Private & Privileged Information

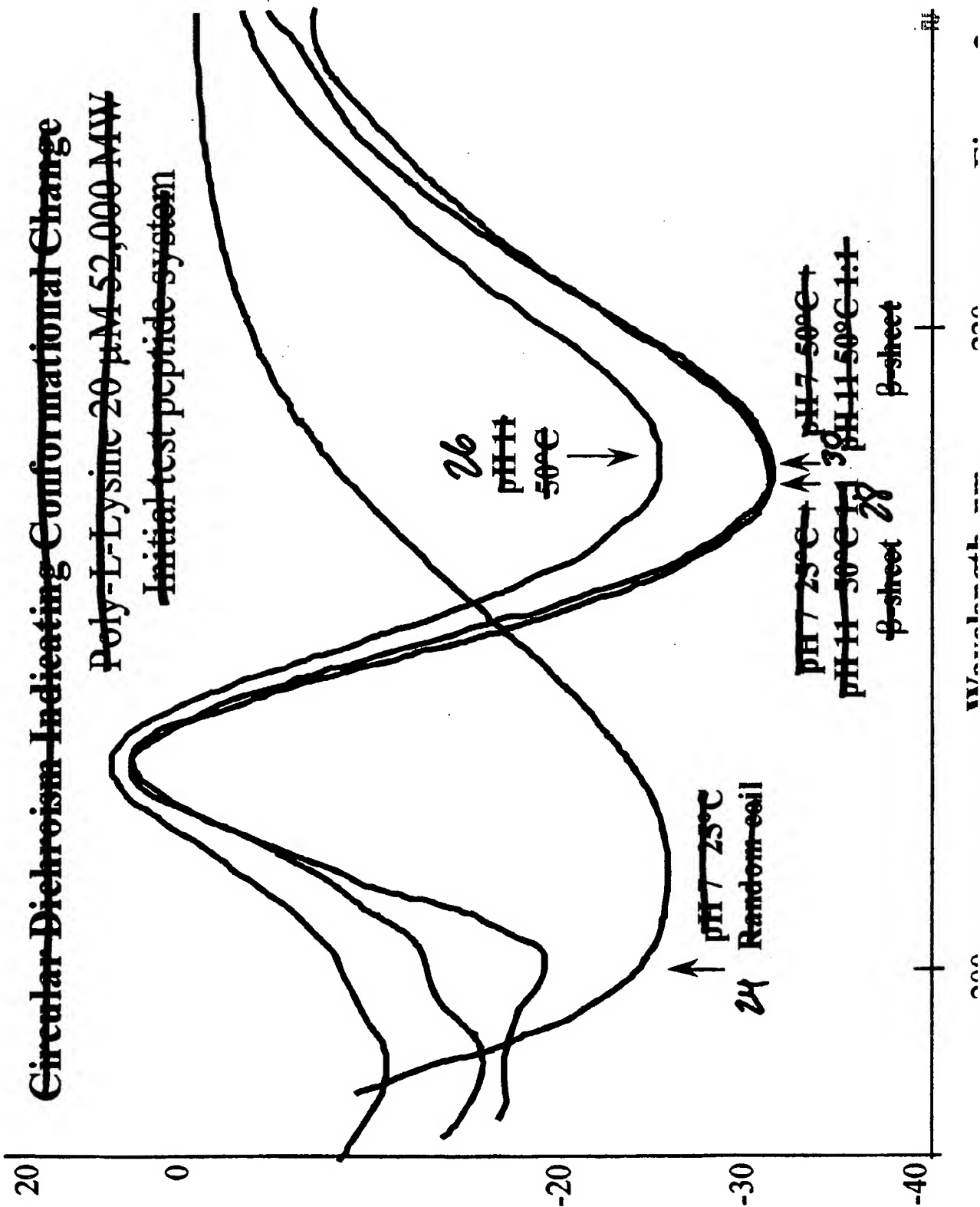
TSE Detection Schema



Circular Dichroism Indicating Conformational Change

Poly-L-Lysine 20 μ M 52,000 MW

Initial test peptide system



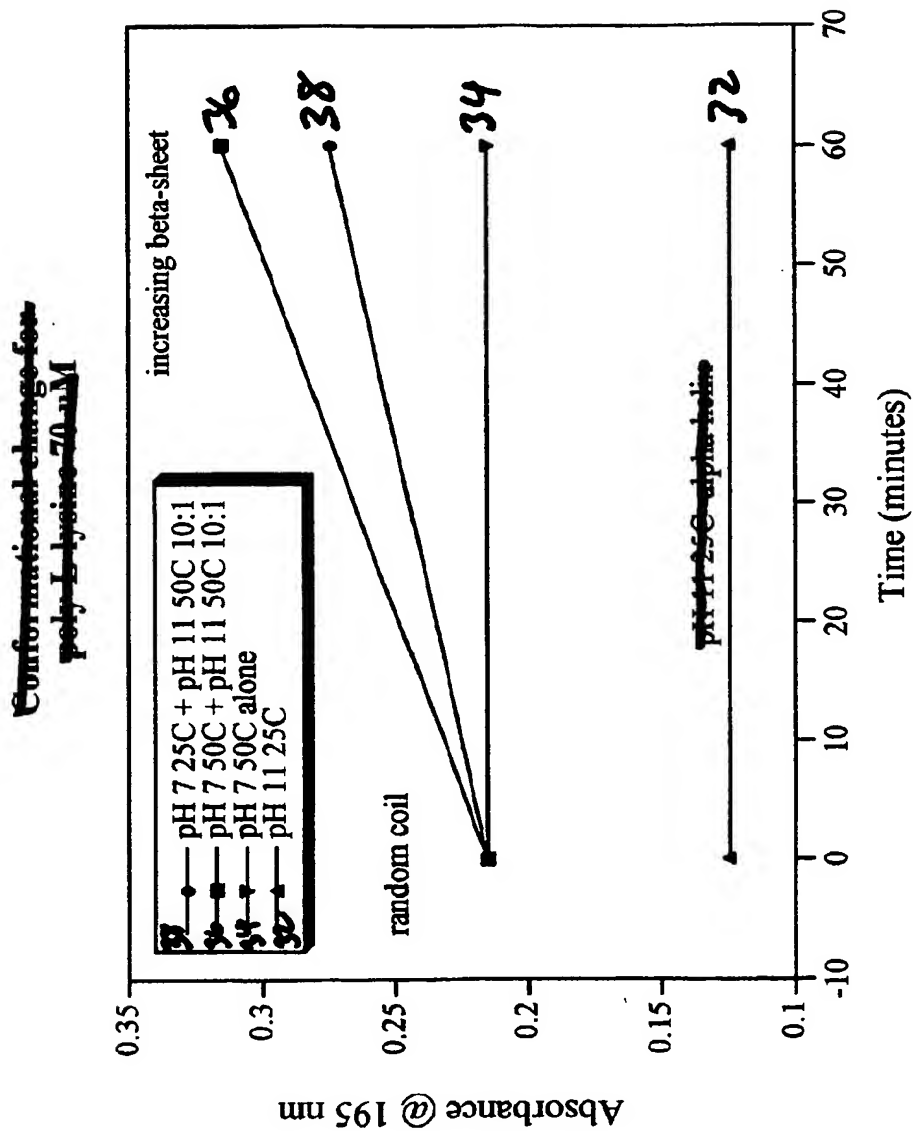


Figure 4

Temperature (°C)	25 °C	50 °C
pH 7 alone	Random coil	Random coil
pH 11 alone	alpha-helix	beta-sheet
pH 7 + pH 11	beta-sheet	beta-sheet
pH 11 at 25 °C + pH 11 at 50 °C	Random coil	-----

Figure 5

~~The data are from previous experiments for proximal and distal locations in an α -helical bundle structure undergoing conformational change.~~

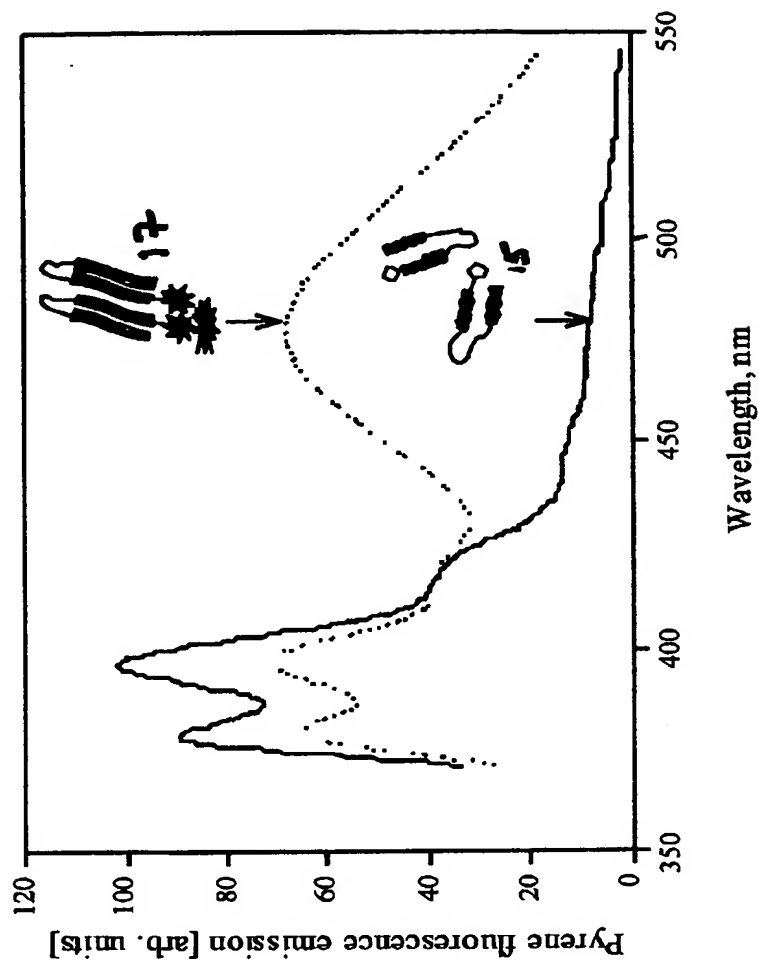
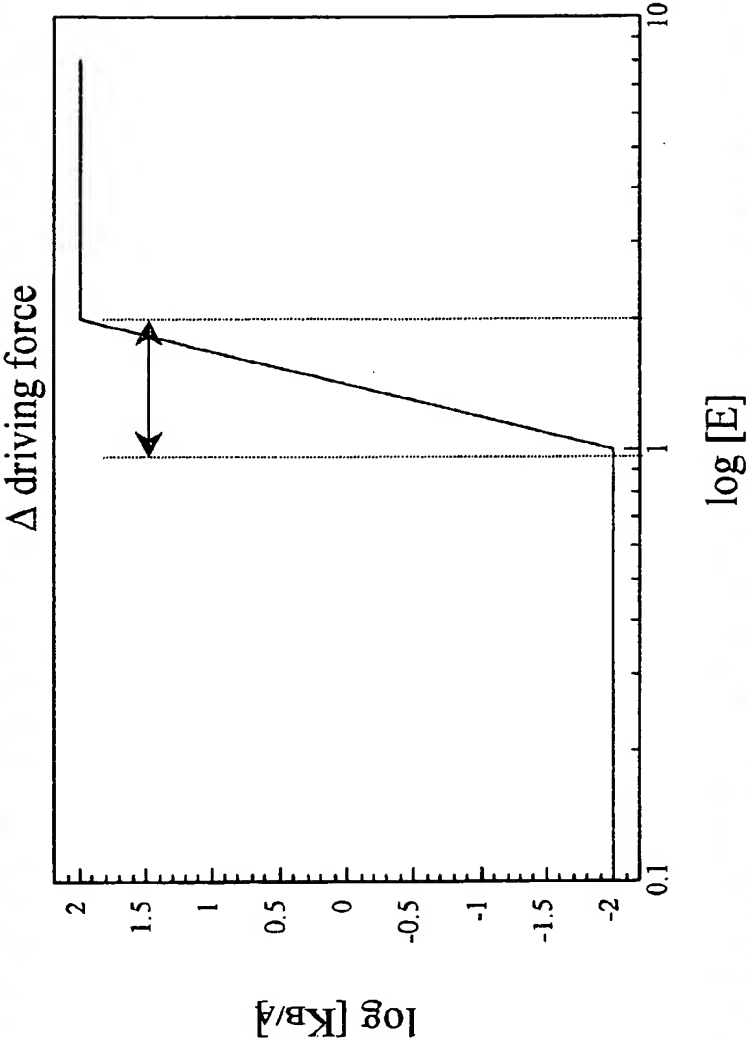


Figure 6

~~The spectra shown are for pyrenic excimer formation at 480 nm, but other probes can be used.~~

~~Engineering considerations for sensor design~~



~~The driving force must be commensurate with the energetic difference between the two conformational states~~

The process is driven by a differential interaction of the target peptide E, with the two conformations of the test P-P molecule.

Figure 7

Overview of Prions

Fig. 8

Transmissible Spongiform Encephalopathies (TSEs)

Scrapie

Mad Cow (BSE)

Creutzfeldt-Jakob Disease (CJD)

Chronic Wasting Disease (CWD)

nvCJD

"Folding disease": characterized by

proteins with destabilizing

conformers which tend to aggregate

and form toxic plaques in brain

tissue

Normal PrP Protein

- ~~cell-surface metallo-glycoprotein~~
- ~~mostly α -helix and loop structure~~
- ~~soluble~~
- ~~expressed in the CNS and lymphatic~~

Proposed Function

~~anti-oxidant~~

~~cellular homeostasis~~

Disease Process

~~resistant to proteases~~

~~mostly β structure~~

~~What goes wrong?~~

~~Conformational change~~

~~leads to aggregation,~~

~~neurotoxic fibril formation~~

~~and plaque deposition~~

~~Prion protein~~

Fig. 9

Dendrimer Target:

Amplification of signal and propagation of conformational change,

without aggregation.

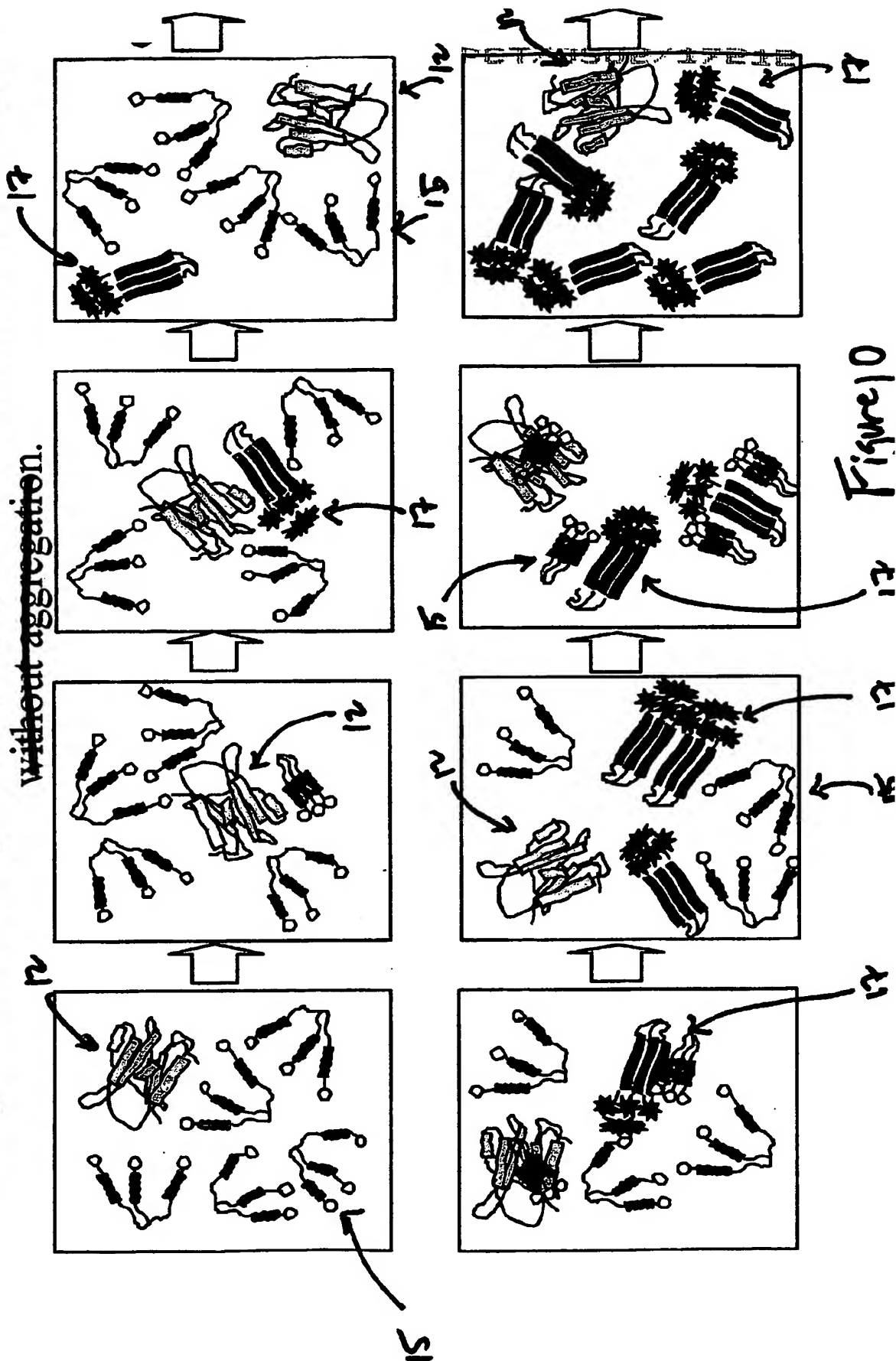
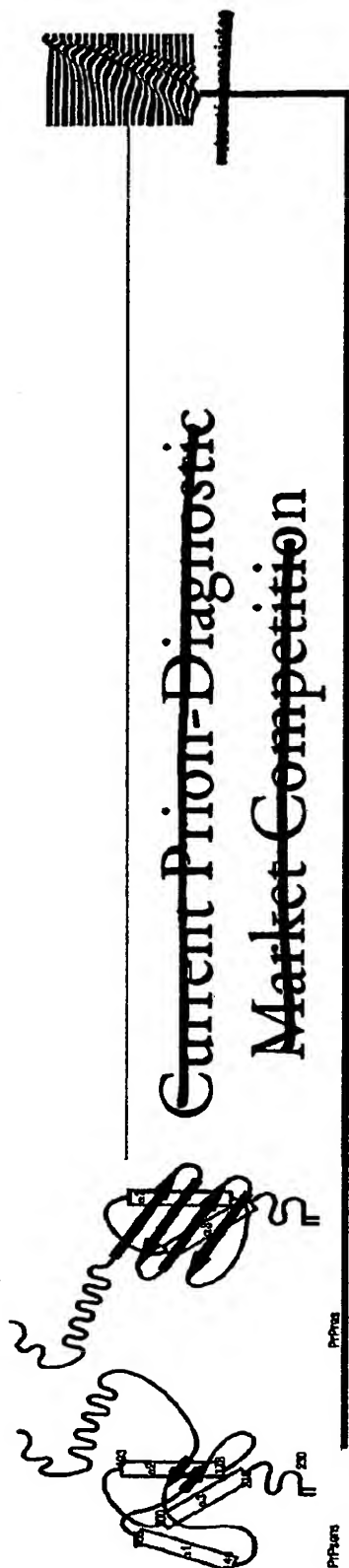


Figure 10



Current Prion-Diagnostic Market Competition

Figure 11

Three European Union certified tests from:

- ~~Prionics (Swiss): Western blot uses monoclonal antibody to detect PrP in brain tissue from dead animals in 7 to 8 hours~~
- ~~Enfer Scientific (Irish): ELISA based, testing on spinal cord tissue from dead animals in under 4 hours~~
- ~~CEA (French): sandwich immunoassay using two monoclonals on brain tissue collected after death in under 24 hours~~

EU Test Results

Tests Evaluated	Sensitivity <i>true positive</i>	Specificity <i>true negative</i>	Detection Limit*^
Prionics Check	100%	100%	10 ⁻¹
Enfer	100%	100%	~126 LD50/g 10 ^{-1.5}
CEA	100%	100%	~70 LD50/g 10 ^{-2.5}
E.G. & G. Wallac	70%	90%	~7 LD50/g 10 ⁰ ~1259 LD50/g

* Material used to prepare dilutions was bovine nervous tissue titrated in mice at 10^{3.1} mouse i.c. LD50/g of tissue. (= 1259 LD50/g)

^ An infectious dose is designated to be 10³ PrP monomers per Brown *et al.* (1994) Ann. Neurology 35:513-529

~~Private & Privileged Information~~

Figure 12

~~Selected PRP Sequence~~ ~~Species Comparison~~

	104	110	120	130	140
<i>Human</i>	KPK	TN	MKH	MAGAAAGAVVGG	LGGLGGYMLGSAMSRP
<i>Hamster</i>	KPK	TN	MKH	MAGAAAGAVVGG	LGGLGGYMLGSAMSRP
<i>Mouse</i>	KPK	TN	LK H	VAGAAAGAVVGG	LGGLGGY LGSAMSRP
<i>Bovine</i>	KPK	TN	MKH	VAGAAAGAVVGG	LGGLGGY LGSAMSRP
<i>Elk</i>	KPK	TN	MKH	VAGAAAGAVVGG	LGGLGGY LGSAMSRP
<i>Deer</i>	KPK	TN	MKH	VAGAAAGAVVGG	LGGLGGY LGSAMSRP

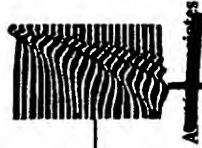
Figure 13

19-mer *KPKTNMKHMAAGAAAGAVV Seq. 1d. No. 19
 14-mer *MKHMAAGAAAGAVV Seq. 1d. No. 14.
 lys-pro-lys-thr-asn-met-lys-his-met-ala-gly-ala-ala-gly-ala-val
 (—With and without the conjugate *pyrene butyric acid)

Figure 14

~~Private & Privileged Information~~

23



Peptide Concentration Effect

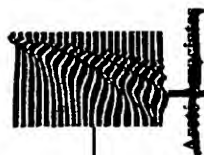
- ~~Fluorescence spectra recorded for 5, 10 and 150 μ M (from bottom to top) are shown as an example of the effect of increasing peptide conc. The highest conc. at 800 μ M is not in view.~~
- ~~Data were collected over time from 1 h to a week with no experimental changes observed after 24 h.~~



~~Private & Privileged Information~~

24

Figure 15



~~Fluorescence Study Finding~~

- ~~Fluorescence spectra normalized to the intensity at 378 nm for the initial scan were collected for the four μ M peptide concentrations: 5 (1), 10 (2), 150 (3) and 800 (4)~~
- ~~Spectrum for the highest peptide concentration, 800 μ M (4), is different, and the suspected excimer emission with maximum at \sim 460 nm can be observed.~~

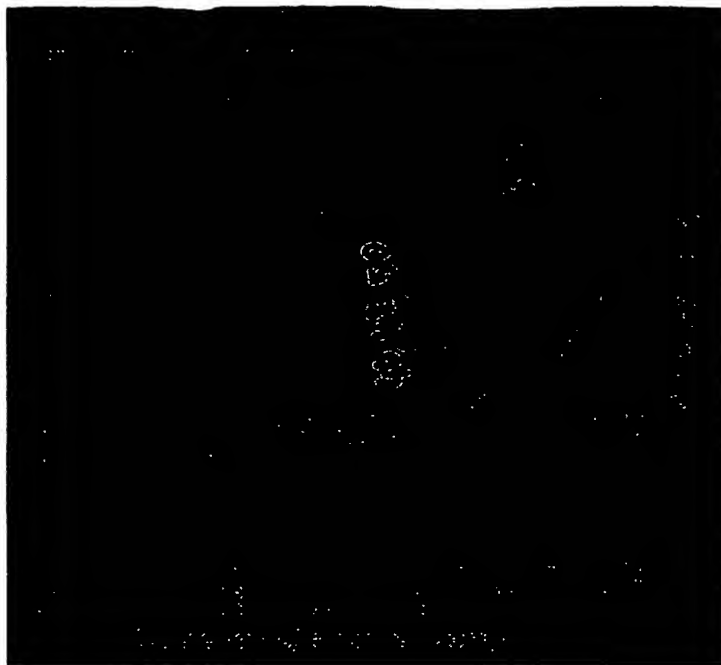
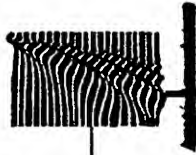


Figure 16

~~Private & Privileged Information~~

22



~~Pyrene's Excitation of Fluorescence~~

- ~~The excitation of fluorescence
for the labeled peptide
provides encouraging evidence.~~
- ~~Current experiments were
performed with the excitation
wavelength at 365 nm to see
excimer emission at 460nm.~~
- ~~However, excitation at 348 nm
increases the fluorescence
signal by over 100 times with
no other modifications or
signal amplification.~~

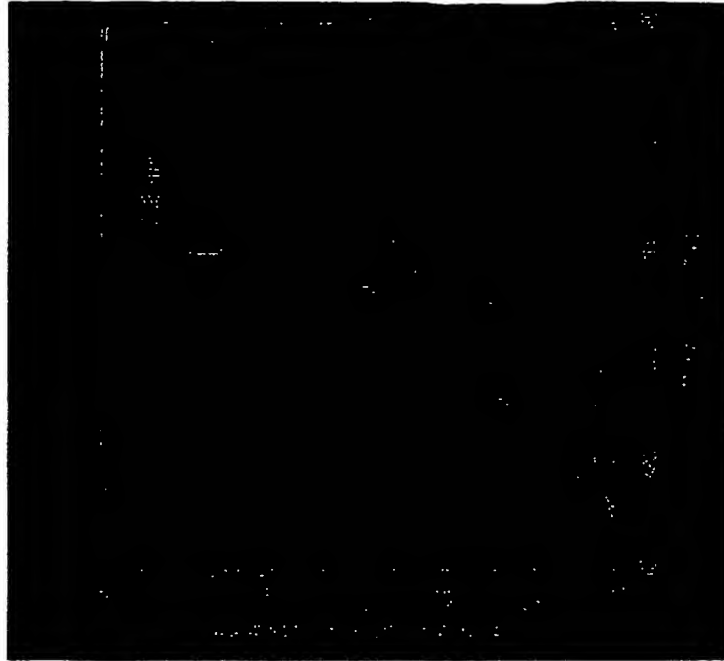


Figure 17

~~Private & Privileged Information~~

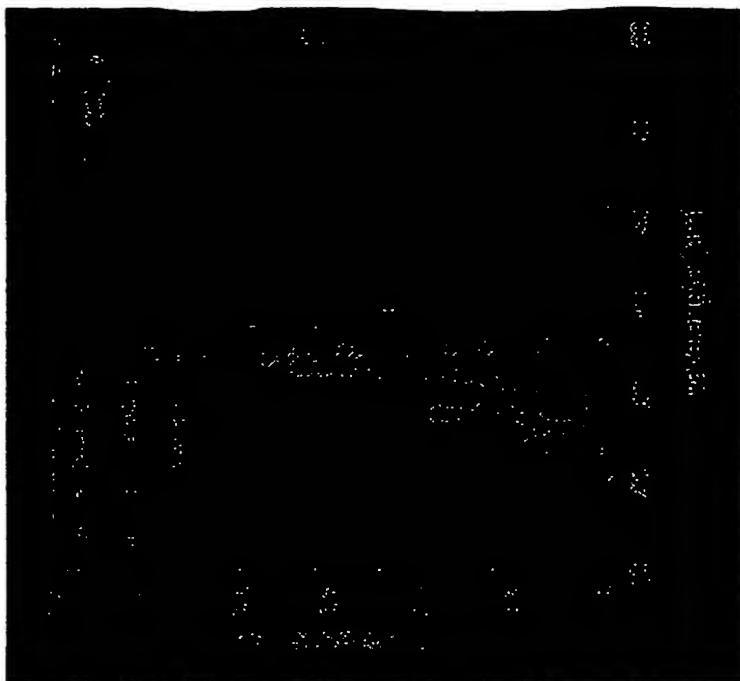
Excitation Spectra for Fluorescence

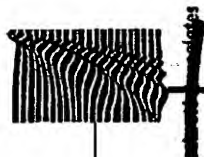
- To confirm that the pyrene conjugate was responsible for both the major 398 nm emission as well as the one at 460 nm, the excitation spectra for fluorescence at 398 nm and at 460 nm were recorded.
- Both excitation spectra are nearly identical with a 365 nm maximum confirming that emission at 460 nm is associated with the formation of excimers by two pyrene groups:



Private & Privileged Information

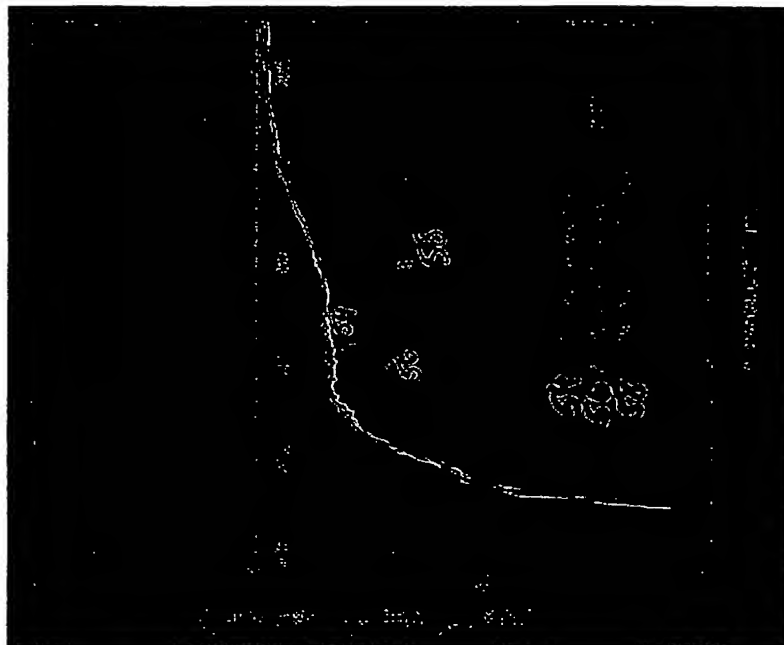
Figure 18





Peptide Stability

- ~~Circular dichroism spectra~~
~~were recorded for a number of~~
~~peptide concentrations ranging~~
~~from 20-100 μ M~~
- ~~GD data show that the 19-mer~~
~~is largely coiled and exhibits~~
~~high thermodynamic stability~~
~~under experimental conditions~~
~~tested (pH, ionic strength, T, ,~~
~~etc)~~
- ~~As expected, the addition the~~
~~organic additions (acetonitrile,~~
~~TFE) encouraged the~~
~~formation of the secondary~~
~~structure~~



Private & Confidential Information

Figure 19

Interaction with Short Analog

Circular Dichroism

- CD spectra were recorded for mixtures of the target peptide (19-mer) and its shorter analog (14-mer).
- Addition of the 14-mer (curves 6) significantly changes the CD spectra of the 19-mer (curves 1-3) indicating strong interactions between these molecules.
- The 14-mer triggers conformational changes in the target peptide. Assembling of the peptide fragments occurred under dilute conditions (11M).

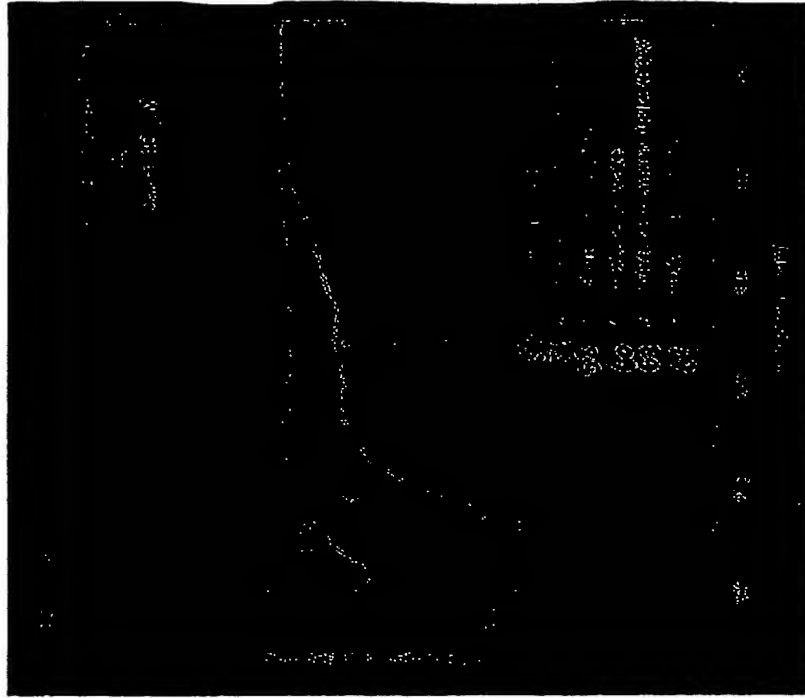


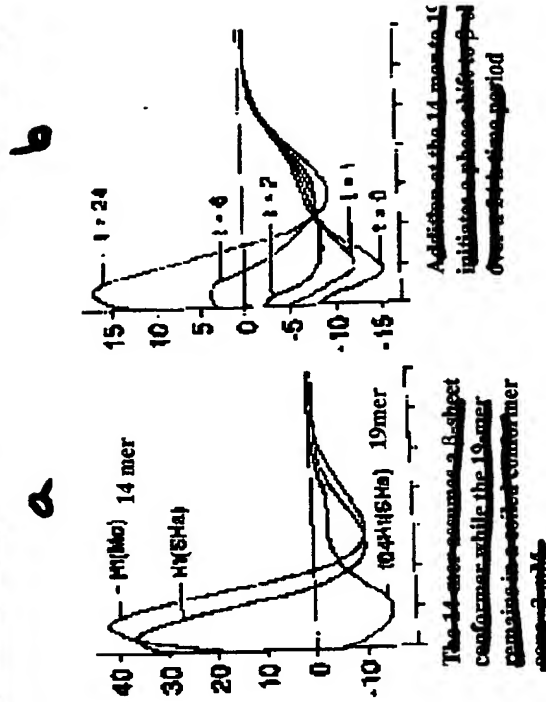
Figure 20

99

Conformational Lability of Peptide

- In good agreement with previous results, it has been shown that the 19-mer exhibits coil-like conformation, whereas the 14-mer is largely β -sheet.

- It has also been shown that the 19-mer can be transformed from the coil-like conformation to a β -sheet conformation through interaction with very small fraction of the 14-mer.



Nguyen J, Baldwin MA, Cohen FE, Prusiner SB (1995) Prion protein peptides induce alpha-helix to beta-sheet conformational transitions. Biochemistry 34:4186-92.

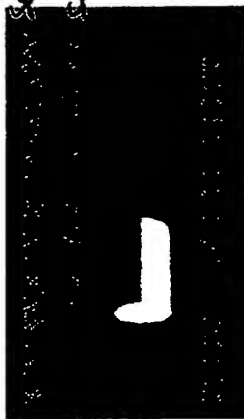
Figure 21. Disclosed Information

Figure 21

Summary of CD Experiments

~~Various secondary structure algorithms were applied to the primary sequences of both peptides. Theoretical secondary structure predictions simulated for 14- and 19-mers show a significant tendency to adopt a partial α -helical conformation:~~

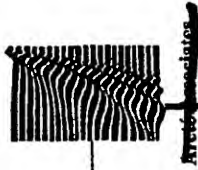
Seq 1d, No. 19
Seq 1d, No. 14



- ~~This, however, does not agree with the CD data.~~
- ~~Conformation of both peptides are clearly concentration-dependent~~
- ~~19-mer exhibits largely a coil conformation, which is stable under a wide variation of the experimental conditions (current results).~~
- ~~14-mer exhibits a transition from coil or hairpin to β -sheet structure depending on concentration.~~
- ~~The 19-mer should be conformationally sensitive to the presence of~~
~~prior-like structures exhibiting 'coil- β -sheet transition'.~~

21

Figure 2c



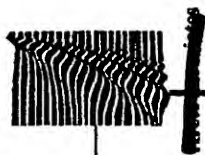
~~Does the peptide self associate?~~

- ~~Can this peptide self associate?~~
 - ~~Yes, with increasing concentration (Curve 1)~~
 - ~~At low concentrations with pH modification to give a net neutral charge and using KCl to screen charge (Curve 2)~~
 - ~~Also at low concentrations with the introduction of "nuclei" acting as a seed or initiator (later charts)~~
- ~~We can optimize the conditions for peptide self association.~~



~~Private & Privileged Information~~

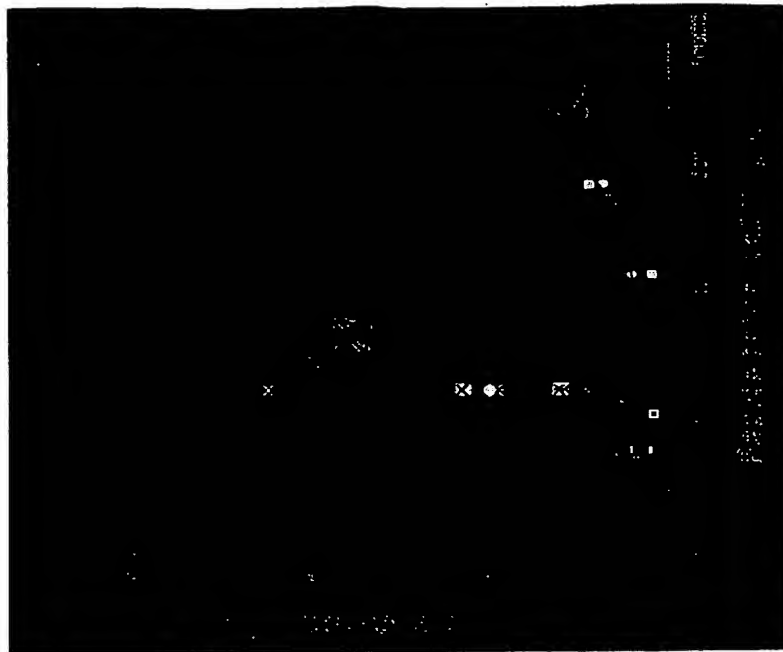
Figure 23



Efficiency of Excimer Formation

under low concentrations

- The ratio of fluorescence intensities as measured at 378 nm (I_M) and at 460 nm (I_E) was chosen to monitor the self association as a function of peptide concentration at 25 °C:
- Curve 1 - 0.1 M TRIS, pH 6.8
- Curve 2 - 0.1 M TRIS, pH 10.11 in the presence of KCl (100=500 mM).
- Screening of the electrostatic interactions (pH 10) encourages self association at extremely low concentration (10^{-4} M).



Private & Privileged Information

Figure 24

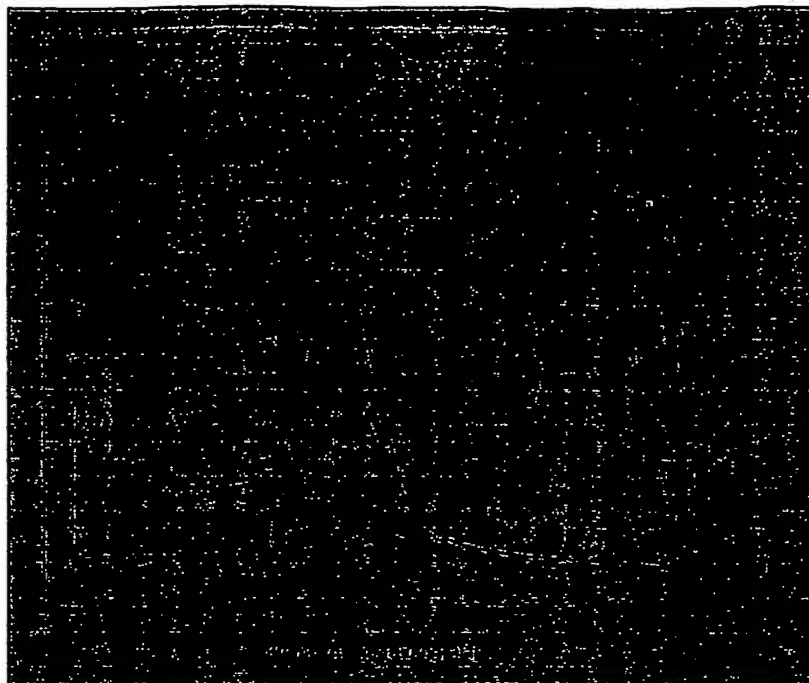


~~Catalytic Conformational Transition~~

Effect of Nuclei on Self-Association

- ~~Peptide stock solutions of 200 and 800 μ M (without and with associates, inset) were~~

~~-O-0.1 M TRIS pH 10
 -□-0.1 M TRIS pH 10, 150 mM KCl
 -△-0.1 M TRIS pH 10, 500 mM KCl
 -■-0.1 M TRIS, pH 8, 300 mM KCl
 -▲-0.1 M TRIS pH 8, 500 mM KCl
 -●-0.1 M TRIS pH 10, 15 % acetonitrile
 -■-0.1 M TRIS pH 10, 30 % acetonitrile
 -▲-0.1 M TRIS pH 10, 15 % acetonitrile, 300 mM KCl
 -◆-0.1 M TRIS pH 10, 30 % acetonitrile, 300 mM KCl
 -●-0.1 M TRIS pH 10, 10 % TFE
 -■-0.1 M TRIS pH 10, 20 % TFE
 -▲-0.1 M TRIS pH 10, 10 % TFE, 300 mM KCl
 -◆-0.1 M TRIS pH 10, 20 % TFE, 300 mM KCl~~



~~Privileged Information~~

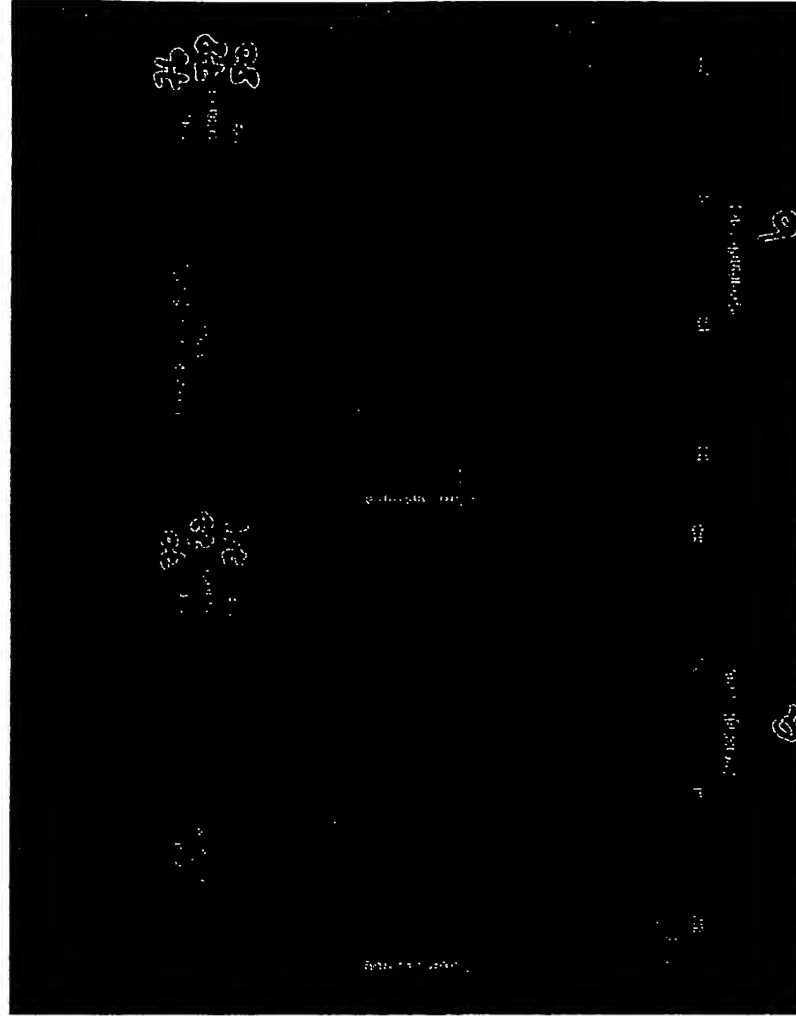
Figure 25

34

Interaction with Short Analog Fluorescence

- Small additions of the 14 mer peptide significantly encouraged the self assembling of the 19 mer target peptide.

- Association was monitored by the appearance of the excimer emission at 460 nm.

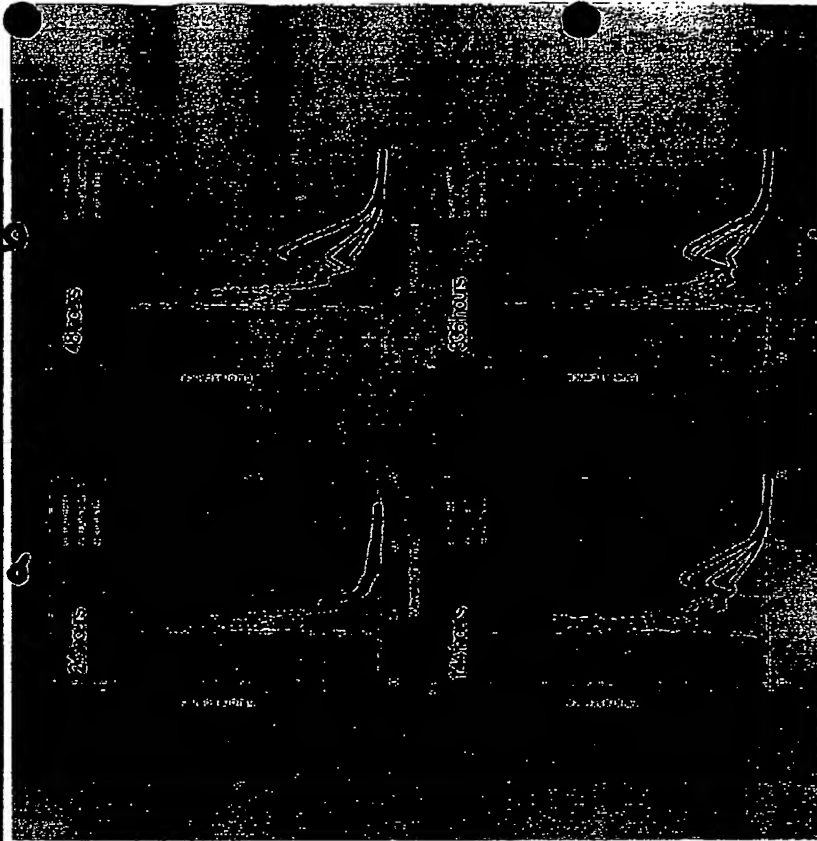


Private & Privileged Information

Figure 26

~~Effect of Nuclei on Self-Association~~ ~~RAW DATA~~

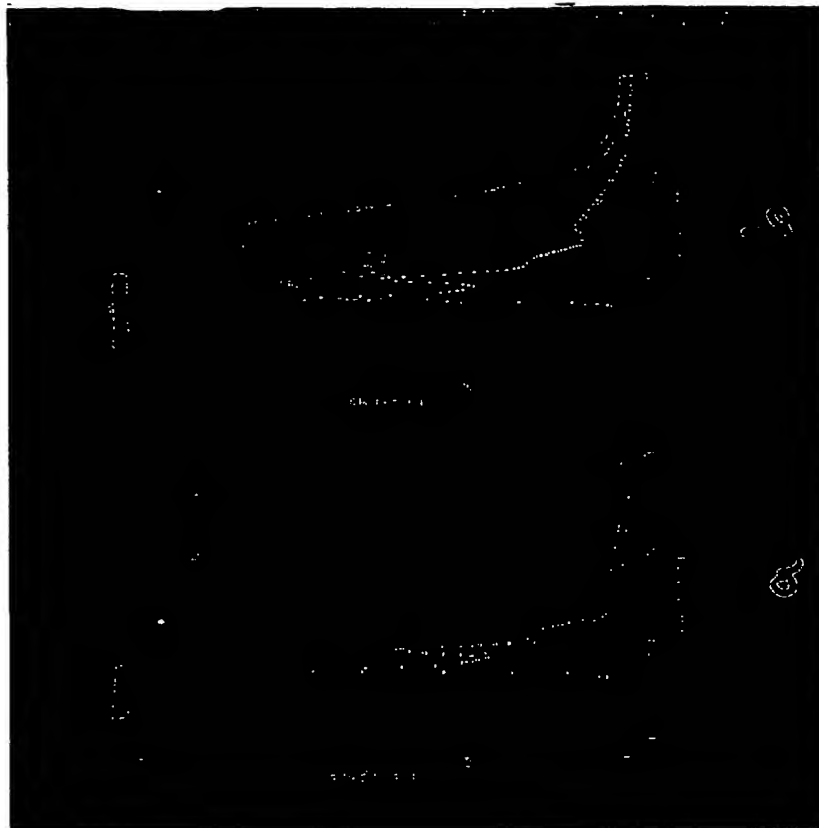
- ~~Effect of pH, temperature, ionic strength, organic additions etc. on kinetics of peptide association were monitored.~~
- ~~Fluorescence intensities as measured at 378 nm (monomeric) and 460 nm (associates) were used to characterize the self-association of the peptide, I_E/I_M ratio.~~



~~Private & Privileged Information~~ **Figure 27** 25

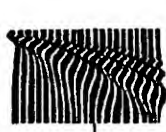
~~Catalytic Conformational Transition - Effect of Nuclei on Self Association~~

- Insoluble fraction of the peptide was extracted and dissolved in organic solvent (methanol/ethanol/DMAc)
- Fluorescence of the "insoluble" portion shows high level of peptide association (I_F/I_M)
- Small aliquot of the "insoluble" were added to the 20 μ M peptide solutions
- Presence of nuclei significantly increased the efficiency of peptide association



~~Private & Confidential Information~~

Figure 28





Generalized Dendrimer Structure

KPKTNMKHMAAGAAAGAVV

lys-pro-lys-thr-asn-met-lys-his-met-ala-gly-ala-ala-gly-ala-val-val

Hydrophilic \longrightarrow *hydrophobic*

spacer-K-P-K-T-N-M-K-H-M-A-G-A-A-A-G-A-V-V-

spacer-K-P-K-T-N-M-K-H-M-A-G-A-A-A-G-A-V-V-

spacer-K-P-K-T-N-M-K-H-M-A-G-A-A-A-G-A-V-V-

Seq. Id. No. 20

Figure 29

~~Private & Privileged Information~~

Specific Dendritic Structure

~~Loop turn loop or dendrimer to amplify signal and decrease neurotoxicity~~
~~This is the N terminal segment, probable nucleus for β sheet transition~~

~~Proposed back to back #1 This segment + loop region IS infectious what effect will addition of the mirror segment have? 120-104-109-126~~

~~Change to SS or SSS/AAA?~~

~~Val=Val=essential to β sheet formation~~



Fig 30a Amyloidogenic

palindrome

70

Private & Discontinued Information

Figure 30

~~Experimental Device Concept~~

- ~~Proposed optical device provides for a simple experimental setup~~

~~Light source (blue)~~

~~- lamp~~

~~- laser~~

~~- Format sample cell (gray)~~

~~- Photo multiplier (pink)~~

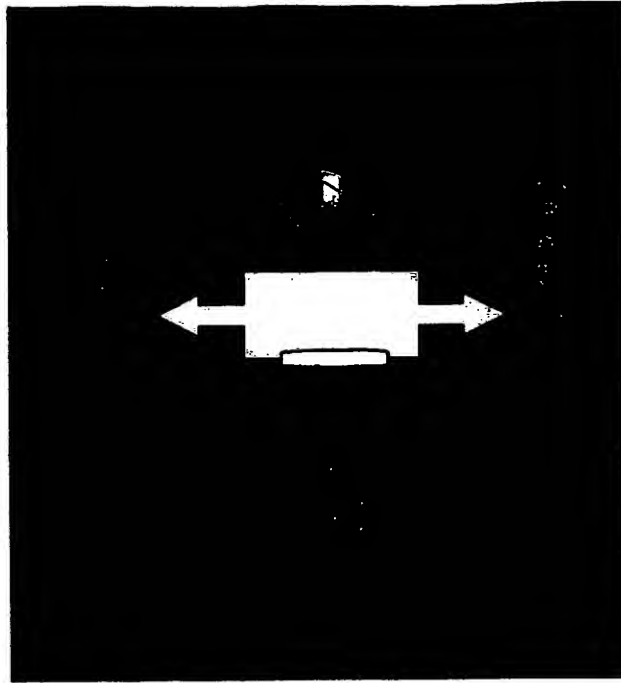


Figure 31

~~Private & Privileged Information~~

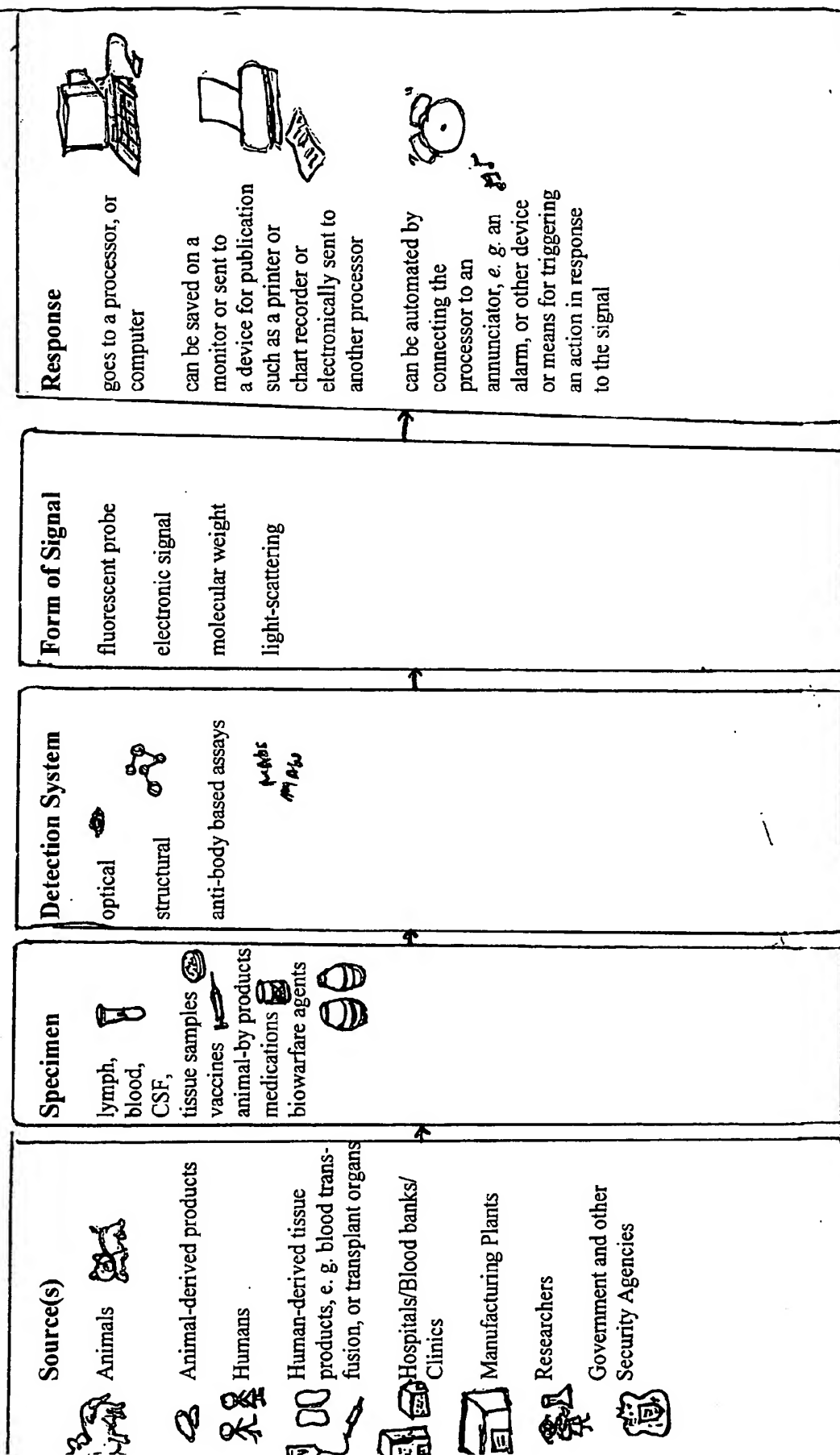


Figure 32

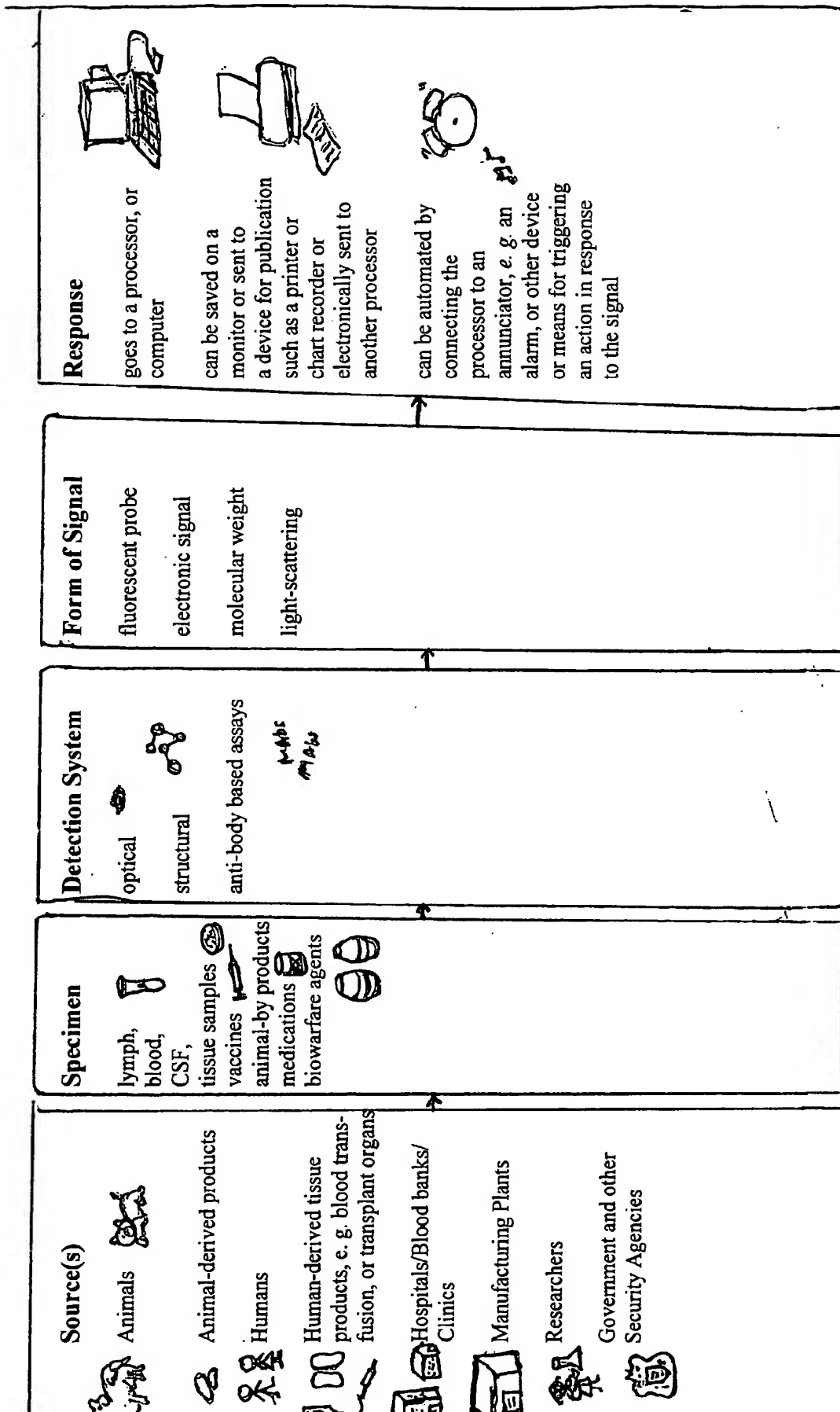


Figure 32

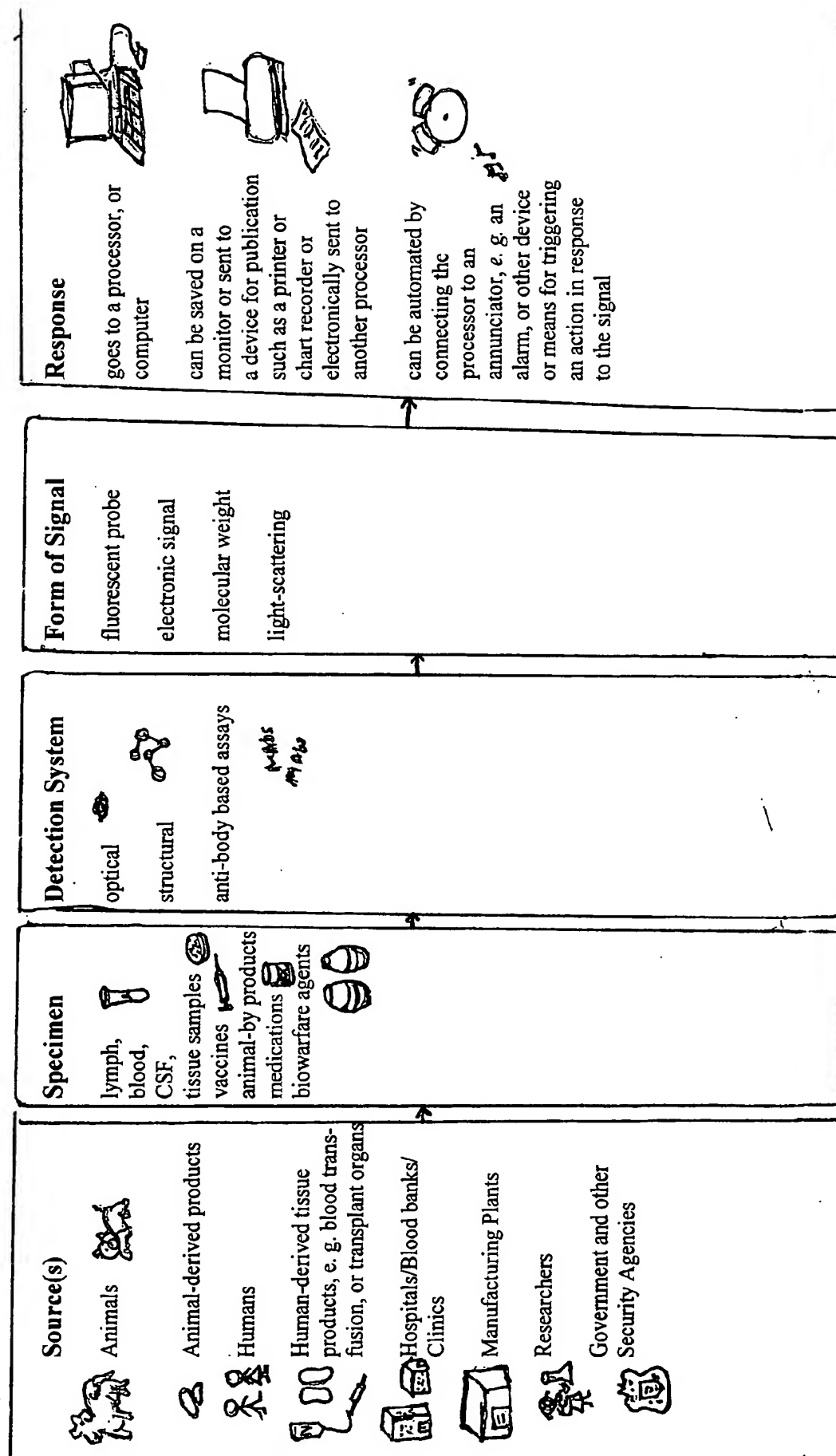


Figure 32

**This Page is Inserted by IFW Indexing and Scanning
Operations and is not part of the Official Record**

BEST AVAILABLE IMAGES

Defective images within this document are accurate representations of the original documents submitted by the applicant.

Defects in the images include but are not limited to the items checked:

☐ **BLACK BORDERS**

☐ **IMAGE CUT OFF AT TOP, BOTTOM OR SIDES**

☐ **FADED TEXT OR DRAWING**

☐ **BLURRED OR ILLEGIBLE TEXT OR DRAWING**

☐ **SKEWED/SLANTED IMAGES**

☒ **COLOR OR BLACK AND WHITE PHOTOGRAPHS**

☐ **GRAY SCALE DOCUMENTS**

☒ **LINES OR MARKS ON ORIGINAL DOCUMENT**

☐ **REFERENCE(S) OR EXHIBIT(S) SUBMITTED ARE POOR QUALITY**

☐ **OTHER:** _____

IMAGES ARE BEST AVAILABLE COPY.

As rescanning these documents will not correct the image problems checked, please do not report these problems to the IFW Image Problem Mailbox.